# SUPPLEMENTARY FIGURE 1

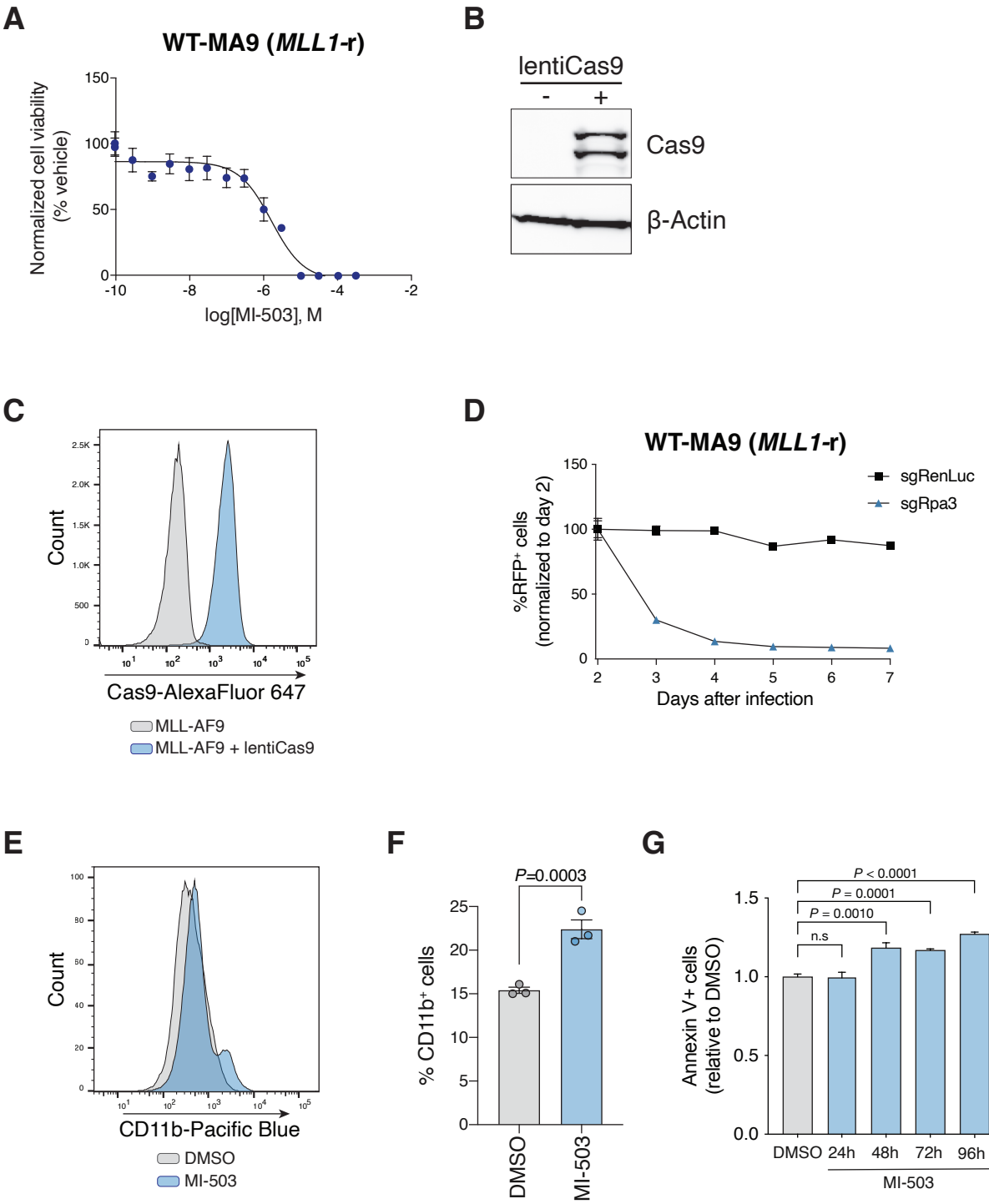


**Supplementary Figure 1. Generation and characterization of Cas9-expressing MLL-AF9 leukemia cells. (A)** Dose response curve analysis of mouse MLL-AF9 leukemia (WT-MA9) cells treated with vehicle (DMSO) or Menin-MLL inhibitor (MI-503) for 96 hours (mean±SEM, n=3 replicates). **(B)** Immunoblot analysis of mouse Cas9-expressing MLL-AF9 leukemia cells. **(C)** Distribution of mouse Cas9-expressing MLL-AF9 leukemia cells determined by intracellular staining of Cas9 and flow cytometry. **(D)** Growth competition assay to test enzymatic activity of Cas9 in mouse MLL-AF9 leukemia cells (mean±SEM, n=3 infection replicates). **(E)** CD11b cell surface expression measured by flow cytometry for vehicle (DMSO, grey) or Menin-MLL inhibitor (MI-503, blue) treatment of mouse MLL-AF9 leukemia cells for 96 hours. **(F)** Quantification of %CD11b positive cells for vehicle (DMSO, grey) or Menin-MLL inhibitor (MI-503, blue) for 96 hours (mean±SEM, n=3 replicates, *P*-value calculated by Student's t-test). **(G)** Quantification of %Annexin V positive cells after treatment with vehicle (DMSO, grey) or Menin-MLL inhibitor (MI-503, blue) at different time points (mean±SEM, n=3 replicates, *P*-value calculated by Student's t-test).

# SUPPLEMENTARY FIGURE 2

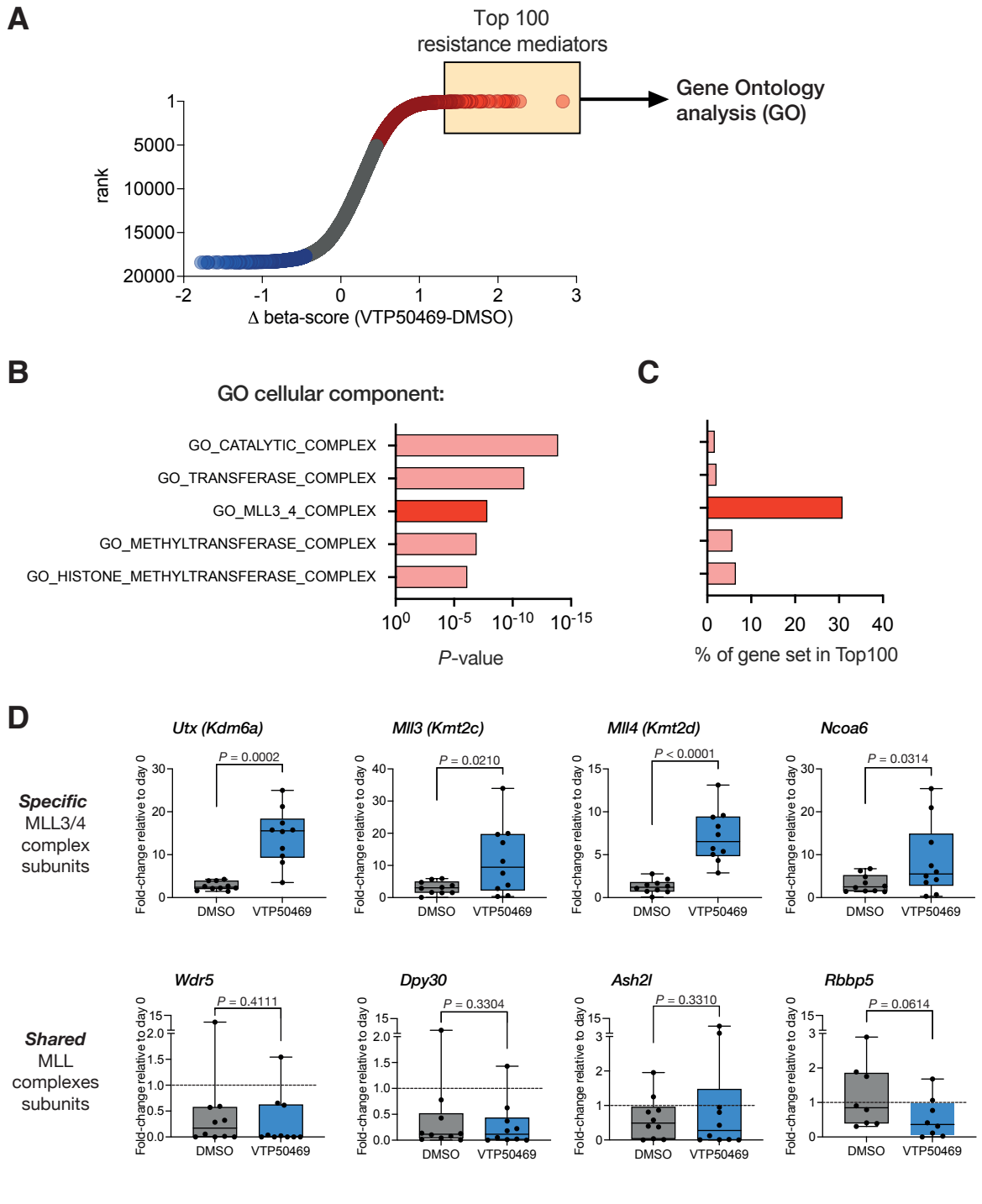


**Supplementary Figure 2. Genome-wide CRISPR screening identifies the MLL3/4-UTX complex as a key determinant of response to Menin-MLL inhibition. (A)** Genome-wide screening data showing gene-level ranking based on differential enrichment of sgRNAs under Menin-MLL inhibitor treatment (VTP-50469) relative to vehicle (DMSO). Differential (Δ) beta-score between VTP-50469 and DMSO conditions was calculated using MaGeCK. A positive Δ beta-score denotes enrichment of specific gene-targeting sgRNAs. A negative Δ beta-score denotes depletion of specific gene-targeting sgRNAs. Red circles denote genes represented by enriched sgRNAs (genes whose inactivation promotes resistance to Menin-MLL inhibition). Blue circles denote genes represented by depleted sgRNAs (genes whose inactivation promotes sensitivity to Menin-MLL inhibition). The top 100 candidate mediators of resistance were selected for gene ontology (GO) analysis. **(B)** Top-scoring GO categories based on *P-values* obtained from GO analysis. **(C)** Percentage of genes within a given gene set that scored among the top 100 candidate mediators of resistance. **(D)** Fold-change of individual sgRNAs relative to $T_0$ from either VTP-50469-treated or DMSO-treated cells (*P*-value calculated by Student's t-test).

# SUPPLEMENTARY FIGURE 3

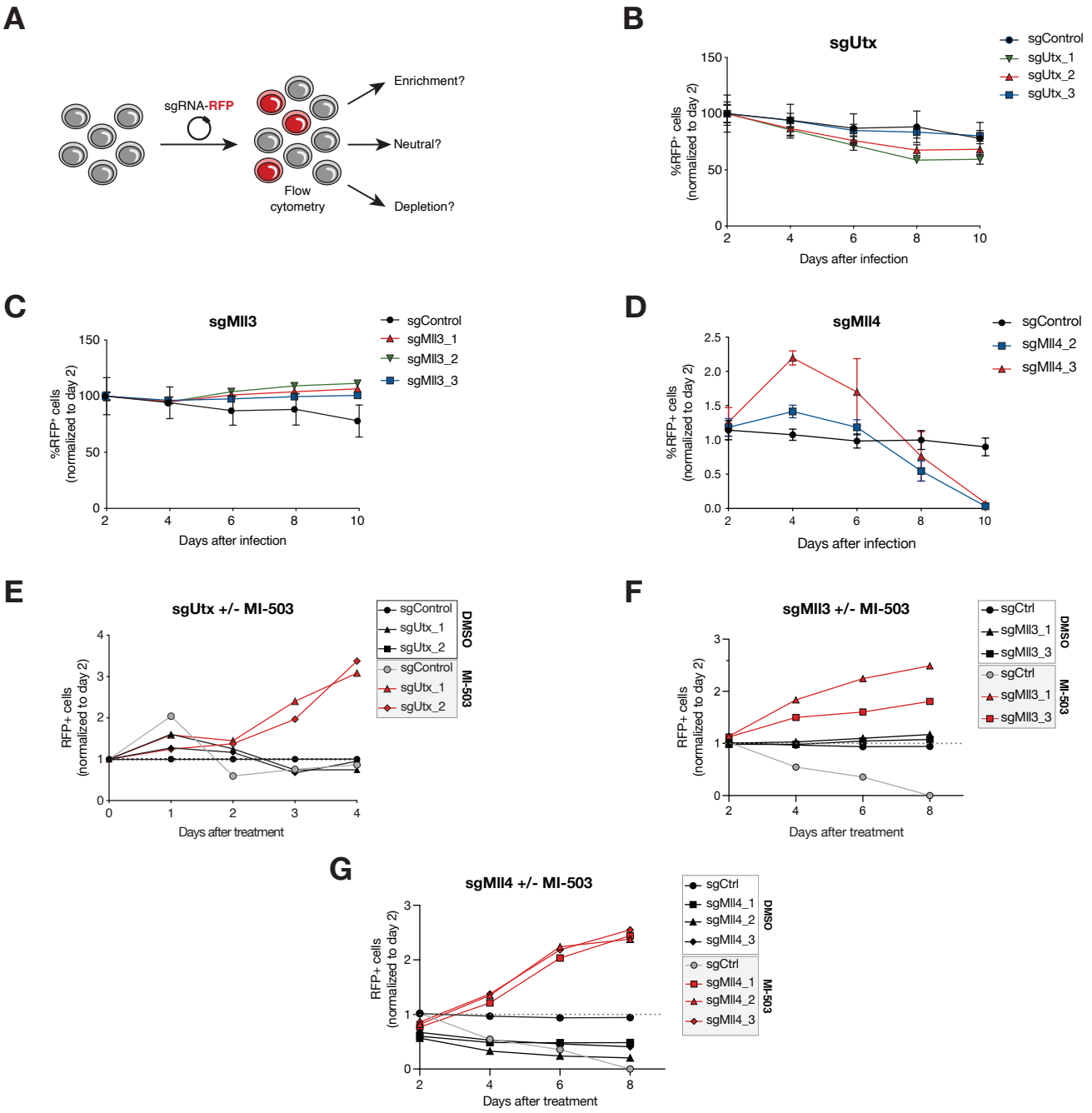


**Supplementary Figure 3. MLL3/4-UTX complex dictates therapeutic response of leukemia cells to Menin-MLL inhibition. (A)** Layout of growth competition assay to assess the effect of genetic loss of *Utx*, *Mll3*, or *Mll4* in MLL-AF9 leukemia cells. **(B)** Growth competition assay in mouse MLL-AF9 cells. Graph shows the relative growth of cells infected with RFP-tagged *Utx* sgRNAs measured by flow cytometry (mean±SEM, n=3 infection replicates). sgControl targets a non-genic region in chromosome 8 as negative control. **(C)** Growth competition assay in mouse MLL-AF9 cells. Graph shows the relative growth of cells infected with RFP-tagged *Mll3* sgRNAs measured by flow cytometry (mean±SEM, n=3 infection replicates). sgControl targets a non-genic region in chromosome 8 as negative control. **(D)** Growth competition assay in mouse MLL-AF9 cells. Graph shows the relative growth of cells infected with RFP-tagged *Mll4* sgRNAs measured by flow cytometry (mean±SEM, n=3 infection replicates). sgControl targets a non-genic region in chromosome 8 as negative control. **(E)** Relative percentage of sgUtx-expressing (RFP+) cells over time after transduction of mouse MLL-AF9 cells treated with vehicle (DMSO) or Menin-MLL inhibitor (MI-503) (mean±SEM, n=3 infection replicates). **(F)** Relative percentage of sgMll3-expressing (RFP+) cells over time after transduction of MLL-AF9 cells treated with vehicle (DMSO) or Menin-MLL inhibitor (MI-503) (mean±SEM, n=3 infection replicates). **(G)** Relative percentage of sgMll4-expressing (RFP+) cells over time after transduction of MLL-AF9 cells treated with vehicle (DMSO) or Menin-MLL inhibitor (MI-503) (mean±SEM, n=3 infection replicates).

# SUPPLEMENTARY FIGURE 4

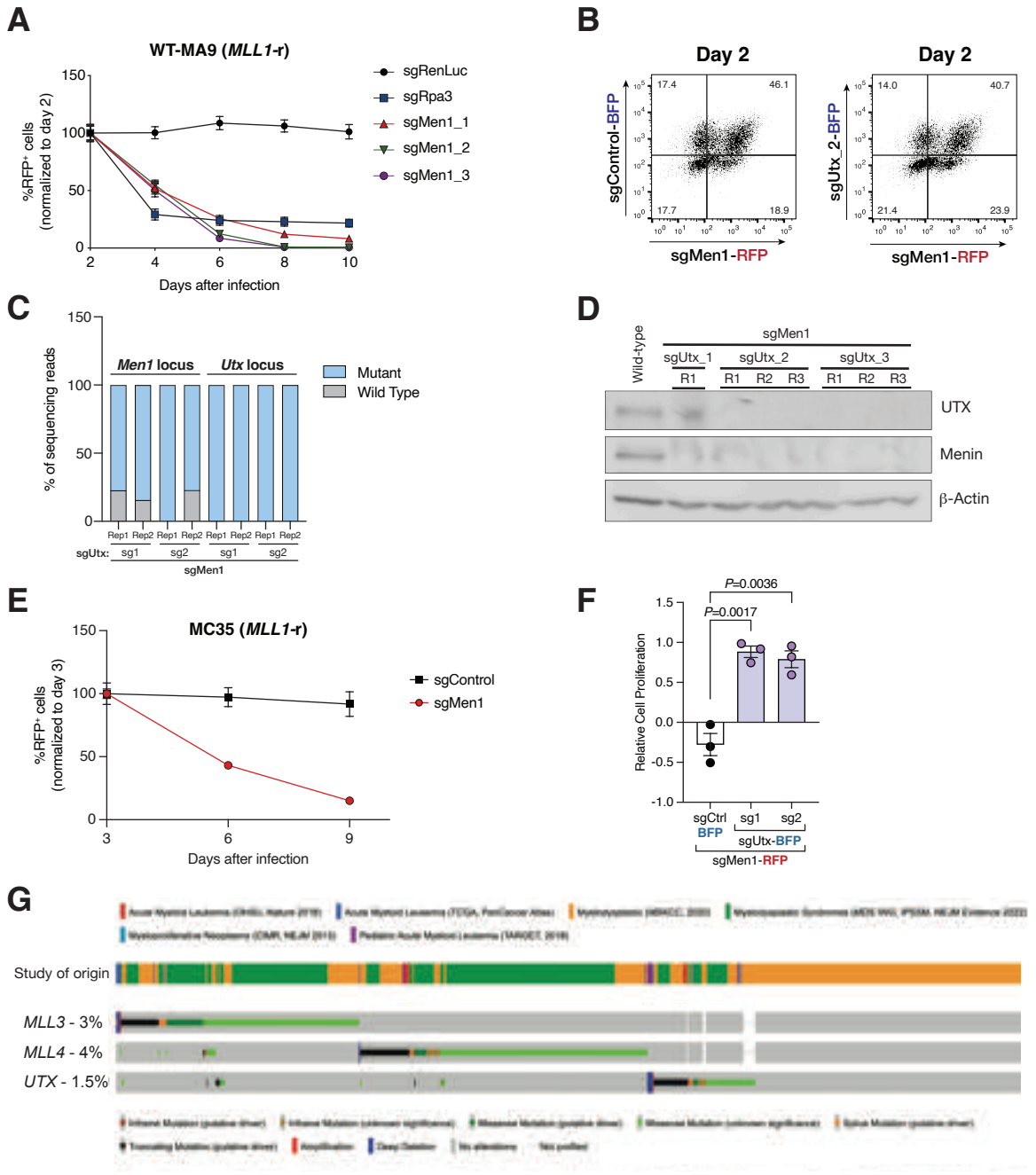


**Supplementary Figure 4. *Utx* deletion suppresses the lethality phenotype associated with *Men1* loss in leukemia. (A)** Growth competition assay in mouse MLL-AF9 cells. Graph shows the relative growth of cells infected with RFP-tagged *Men1* sgRNAs measured by flow cytometry (mean±SEM, n=3 infection replicates). sgRenilla Luciferase (RenLuc) and sgRpa3 were negative and positive controls, respectively. **(B)** Plots from flow cytometry analysis of leukemia cells co-expressing sgMen1-RFP + sgControl-BFP or sgMen1-RFP + sgUtx-BFP at day 2 post-infection. **(C)** Amplicon sequencing results of the mouse *Men1* and *Utx* loci from leukemia cells co-expressing sgMen1 and sgUtx. **(D)** Immunoblot analysis of FACS-sorted leukemia cells co-expressing sgMen1-RFP + sgControl-BFP or sgMen1-RFP + sgUtx-BFP using antibodies against UTX, Menin, and β-actin as loading control. **(E)** Growth competition assay in an independently-derived mouse MLL-AF9 cell line. Graph shows the relative growth of cells infected with RFP-tagged sgRNAs (sgControl and sgMen1) measured by flow cytometry (mean±SEM, n=3 infection replicates). **(F)** Relative proliferation of mouse MLL-AF9 cells is shown as the relative proliferation of double positive cells (sgMen1-RFP + sgUtx-BFP or sgMen1-RFP + sgControl-BFP) to single positive cells (sgMen1-RFP) 9 days post-infection measured by flow cytometry (mean±SEM, n=3 infection replicates, *P*-value calculated by Student's t-test). **(G)** Graphical depiction of frequency and type of genetic alteration in *MLL3* (*KMT2C*), *MLL4* (*KMT2D*), and *UTX* (*KDM6A*) in patients with acute myeloid leukemia (AML), myelodysplastic syndrome (MDS), or myeloproliferative neoplasm (MPN).

# SUPPLEMENTARY FIGURE 5

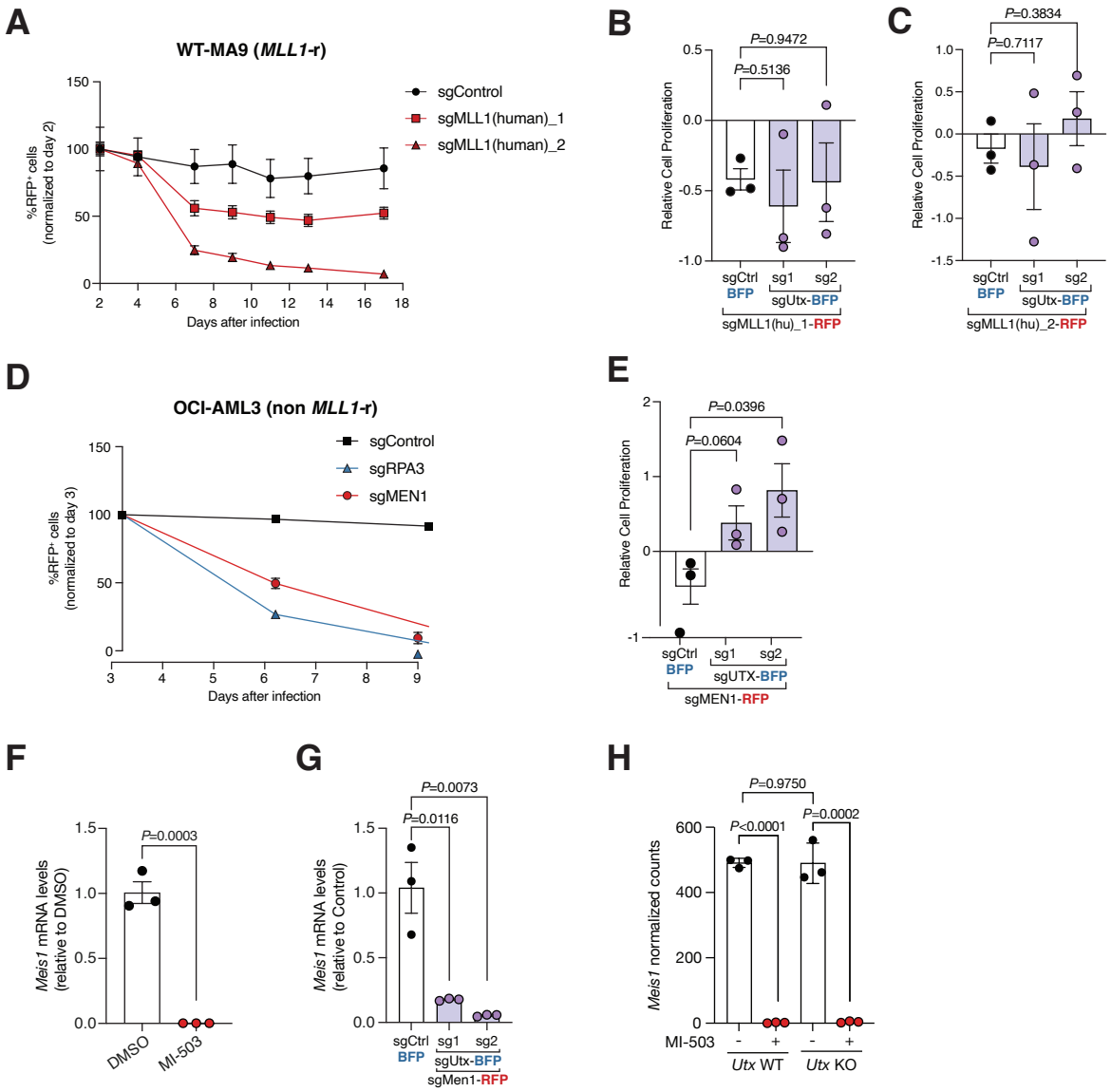


**Supplementary Figure 5. *Men1* and *Utx* epistasis is independent of the MLL-fusion. (A)** Growth competition assay in mouse MLL-AF9 leukemia cells. Graph shows the relative growth of cells, infected with RFP-tagged sgRNAs that target the 5'-end of the human *MLL1* gene present in the MLL-AF9 fusion, measured by flow cytometry (mean±SEM, n=3 infection replicates). **(B)** Relative proliferation of mouse MLL-AF9 leukemia cells is shown as the relative proliferation of double positive cells (sgMLL1(hu)_1-RFP + sgUtx-BFP or sgMLL1(hu)_1-RFP + sgControl-BFP) to single positive cells (sgMLL1(hu)_1-RFP) 16 days post-infection measured by flow cytometry (mean±SEM, n=3 infection replicates, *P*-value calculated by Student's t-test). **(C)** Relative proliferation of mouse WT-MA9 cells is shown as the relative proliferation of double positive cells (sgMLL1(hu)_2-RFP + sgUtx-BFP or sgMLL1(hu)_2-RFP + sgControl-BFP) to single positive cells (sgMLL1(hu)_2-RFP) 16 days post-infection measured by flow cytometry (mean±SEM, n=3 infection replicates, *P*-value calculated by Student's t-test). **(D)** Growth competition assay in human non *MLL1*-r (OCI-AML3) cells. Graph shows the relative growth of cells infected with RFP-tagged sgRNAs measured by flow cytometry (mean±SEM, n=3 infection replicates). **(E)** Relative proliferation of human OCI-AML3 cells is shown as the relative proliferation of double positive cells to single positive cells 20 days post-infection measured by flow cytometry (mean±SEM, n=3 infection replicates, *P*-value calculated by Student's t-test). **(F)** qPCR analysis for *Meis1* expression in mouse MLL-AF9 leukemia cells treated with vehicle (DMSO, black) or Menin-MLL inhibitor (MI-503, red) for 96 hours (mean±SEM, n=3 replicates, *P*-value calculated by Student's t-test). **(G)** qPCR analysis for *Meis1* expression in mouse MLL-AF9 leukemia cells co-expressing sgMen1-RFP and sgUtx-BFP, or a control sgRNA (mean±SEM, n=3 replicates, *P*-value calculated by Student's t-test). **(H)** *Meis1* expression (mean normalized read counts) from $Utx^{WT}$ and $Utx^{KO}$ leukemia cells treated with vehicle (DMSO, black) or Menin-MLL (MI-503, red) for 96 hours (mean±SEM, n=3 replicates, *P*-value calculated by Student's t-test).

# SUPPLEMENTARY FIGURE 6

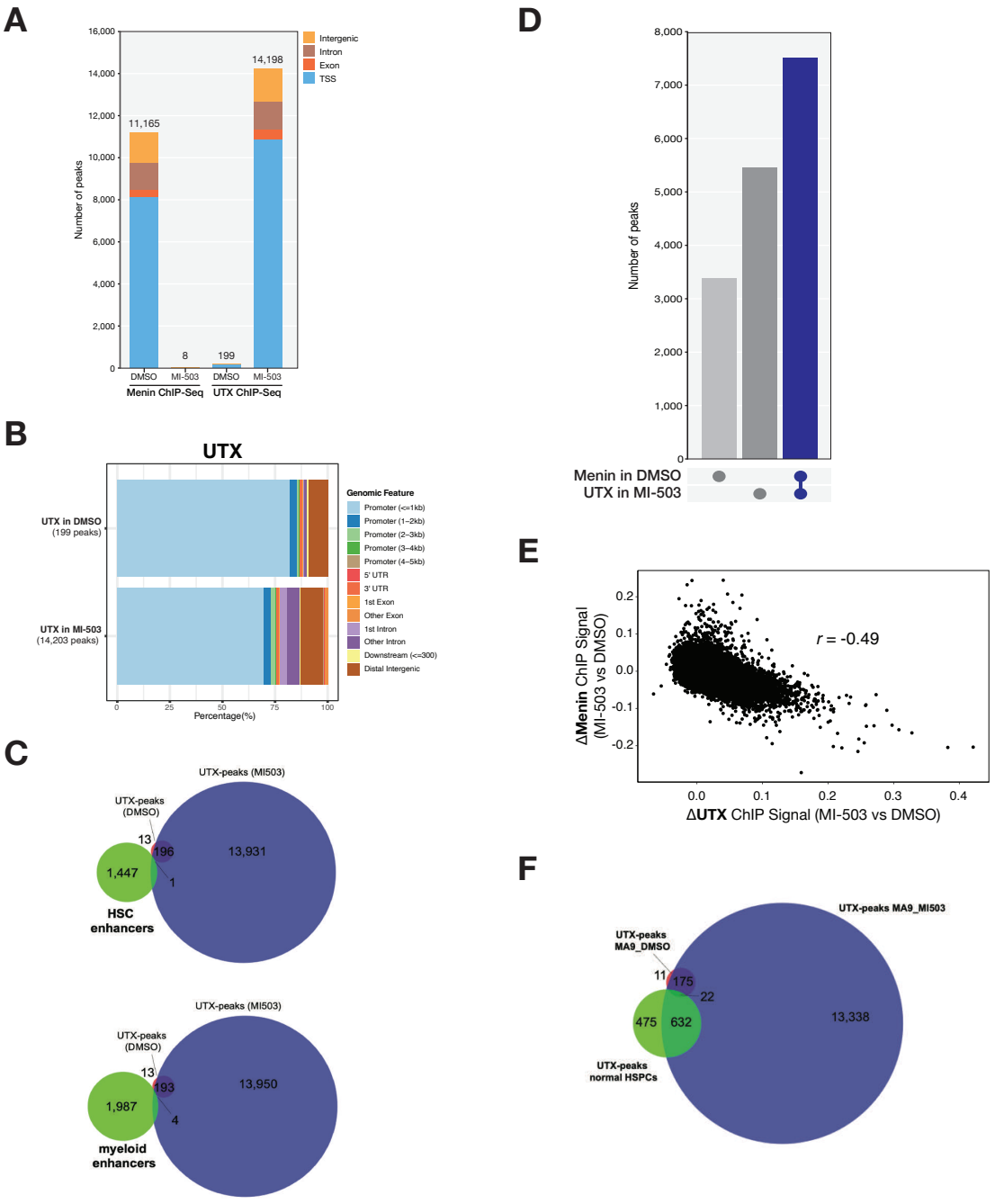


**Supplementary Figure 6. Distinct genomic distribution of Menin and UTX in the context of Menin-MLL inhibition. (A)** Genomic distribution of Menin and UTX ChIP-Seq peaks from mouse MLL-AF9 leukemia cells treated with vehicle (DMSO) or Menin-MLL inhibitor (MI-503) for 96 hours. **(B)** Genomic distribution of UTX ChIP-Seq peaks from MLL-AF9 leukemia cells treated with vehicle (DMSO, top) or Menin-MLL inhibitor (MI-503, bottom). **(C)** Venn diagrams showing overlap analysis of UTX binding peaks from UTX ChIP-Seq of mouse MLL-AF9 leukemia cells treated with vehicle (DMSO, red) or Menin-MLL inhibitor (MI-503, blue) for 96 hours compared to annotated mouse HSC (top, green) and myeloid (bottom, green) enhancers. **(D)** Upset plot showing a comparison between the genomic distribution of Menin ChIP-Seq peaks in vehicle (DMSO, light grey), genomic distribution of UTX ChIP-Seq peaks in Menin-MLL inhibitor (MI-503, gray), and the overlap between UTX ChIP-Seq peaks in MI-503 and Menin ChIP-Seq peaks in DMSO (blue). **(E)** ChIP-Seq normalized reads per 10-kb bin for Menin (MI-503 vs DMSO, y-axis) and UTX (MI-503 vs DMSO, x-axis). Pearson's correlation coefficient is indicated. **(F)** Venn diagrams showing overlap analysis of UTX binding peaks from ChIP-Seq of mouse MLL-AF9 leukemia cells treated with vehicle (DMSO, red) or Menin-MLL inhibitor (MI-503, blue) for 96 hours compared to UTX binding peaks in normal mouse hematopoietic stem and progenitor cells (HSPCs, green).

# SUPPLEMENTARY FIGURE 7

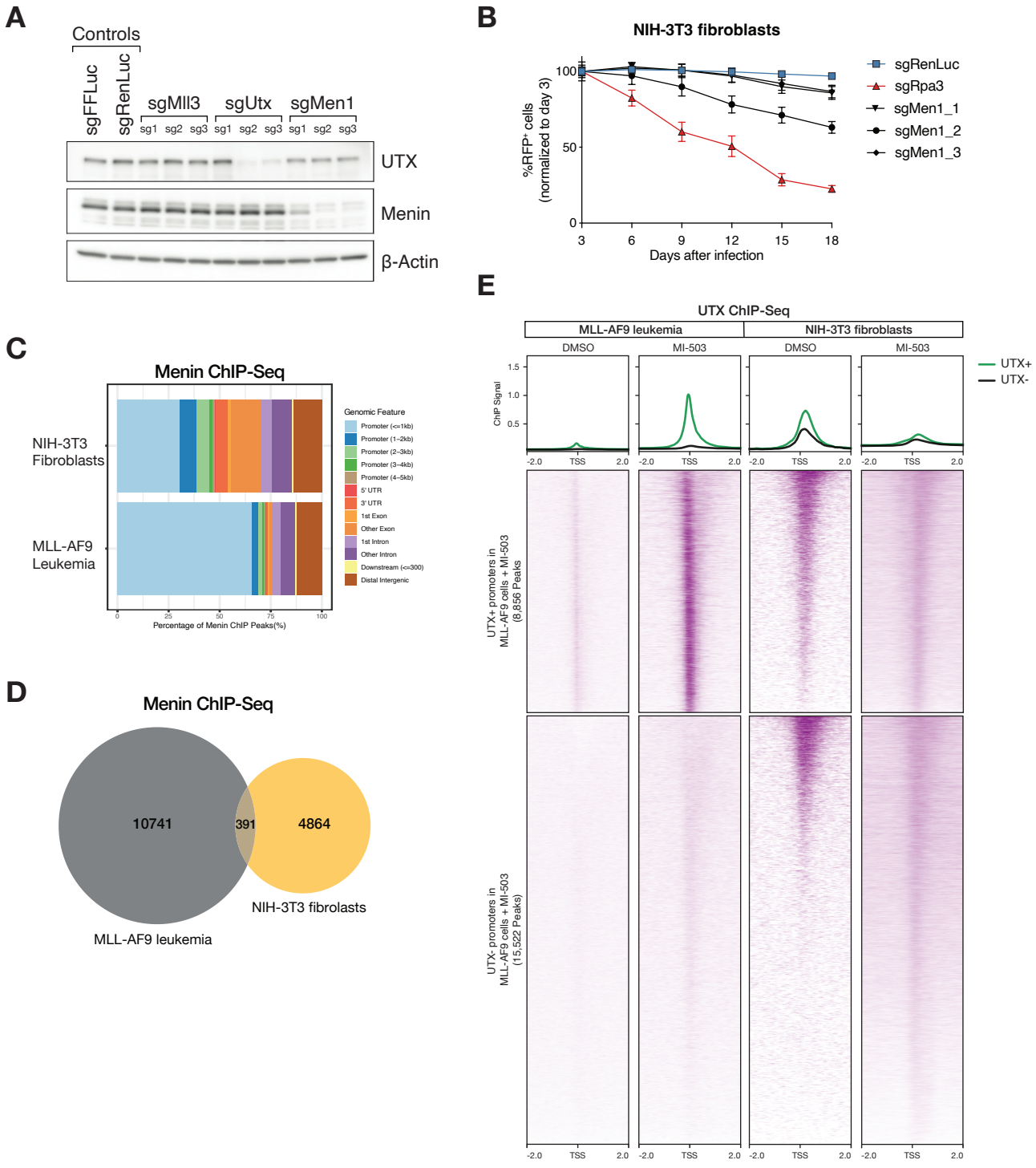


**Supplementary Figure 7. Menin-independent cells do not exhibit chromatin changes associated with the Menin-UTX molecular switch. (A)** Immunoblot analysis of Cas9-expressing mouse fibroblast (NIH-3T3) cells expressing different controls, *Mll3*, *Utx*, and *Men1* sgRNAs using antibodies against UTX, Menin, and β-actin as loading control. **(B)** Growth competition assay in mouse fibroblast cells. Graph shows the relative growth of cells infected with RFP-tagged sgRNAs measured by flow cytometry (mean±SEM, n=3 infection replicates). **(C)** Genomic distribution of Menin ChIP-Seq peaks from mouse fibroblasts (top) or MLL-AF9 leukemia cells (bottom). **(D)** Venn diagram comparing the number of Menin peaks detected in mouse MLL-AF9 leukemia cells (grey) vs. NIH-3T3 fibroblasts (yellow). **(E)** Heatmaps displaying UTX ChIP-Seq signals mapping to a 4-kb window around TSSs. Data is shown for mouse MLL-AF9 cells (left) and mouse fibroblasts (right) treated with vehicle (DMSO) or Menin-MLL inhibitor (MI-503) for 96 hours. Metagene plot represents the average ChIP-Seq signal for UTX at promoters that are enriched for UTX (green) or not (black) in mouse MLL-AF9 cells treated with MI-503.

# SUPPLEMENTARY FIGURE 8

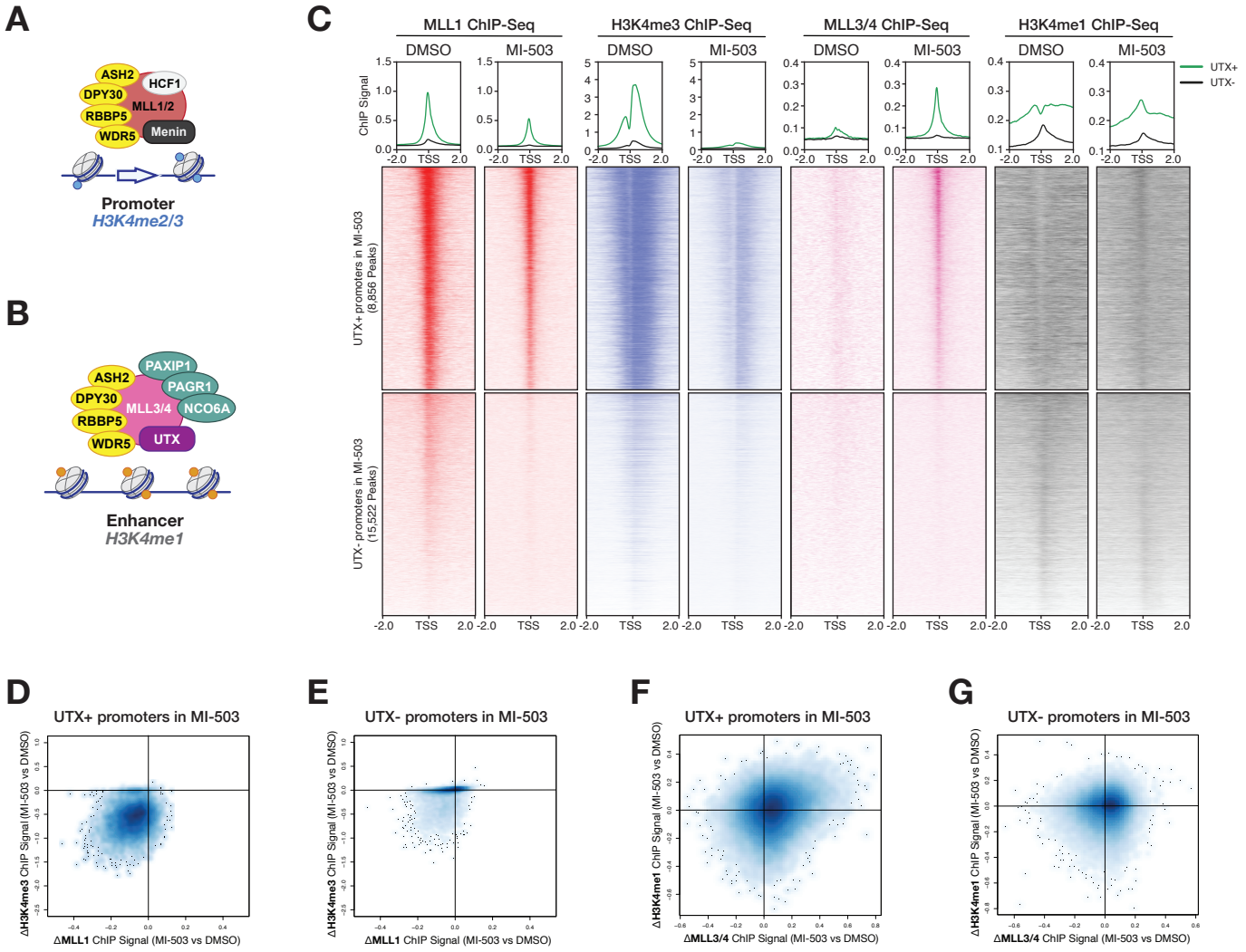


**Supplementary Figure 8. Disruption of Menin-MLL1 interaction leads to targeting of MLL3/4-UTX to sites normally bound by the MLL1-Menin complex. (A)** Schematic representation of the mammalian MLL1 and MLL2 histone methyltransferase complexes. Highlighted in red is the enzymatic subunit of the complex (MLL1 and MLL2 are mutually exclusive). Yellow denotes shared subunits with the MLL3/4 complex. **(B)** Schematic representation of the mammalian MLL3 and MLL4 histone methyltransferase complexes. Highlighted in pink and purple are the enzymatic subunits of the complex (MLL3 and MLL4 are mutually exclusive). Yellow denotes shared subunits with the MLL1/2 complex. Green denotes non-enzymatic subunits of the MLL3/4 complex. **(C)** Heatmaps displaying MLL1 (red) and H3K4me3 (blue) ChIP-Seq signals mapping to a 4-kb window around TSSs. Data is shown for cells treated with vehicle (DMSO) or Menin-MLL inhibitor (MI-503) for 96 hours. Metagene plot represents the average ChIP-Seq signal for each protein at promoters that are UTX+ (green) or UTX- (black). Heatmaps displaying MLL3/4 (pink) and H3K4me1 (grey) ChIP-Seq signals mapping to a 4-kb window around TSSs. Data is shown for cells treated with vehicle (DMSO) or Menin-MLL inhibitor (MI-503) for 96 hours. Metagene plot represents the average ChIP-Seq signal for each protein at promoters that are UTX+ (green) or UTX- (black). **(D)** Density plot showing correlation between H3K4me3 and MLL1 ChIP-Seq signals (MI-503 vs DMSO). Signals correspond to summed signal ±2kb around TSSs that overlap with UTX peaks in MI-503 condition. **(E)** Density plot showing correlation between H3K4me3 and MLL1 ChIP-Seq signals (MI-503 vs DMSO). Signals correspond to summed signal ±2kb around TSSs that do not overlap with UTX peaks in MI-503 condition. **(F)** Density plot showing correlation between H3K4me1 and MLL3/4 ChIP-Seq signals (MI-503 vs DMSO). Signals correspond to summed signal ±2kb around TSSs that overlap with UTX peaks in MI-503 condition. **(G)** Density plot showing correlation between H3K4me1 and MLL3/4 ChIP-Seq signals (MI-503 vs DMSO). Signals correspond to summed signal ±2kb around TSSs that do not overlap with UTX peaks in MI-503 condition.

# SUPPLEMENTARY FIGURE 9

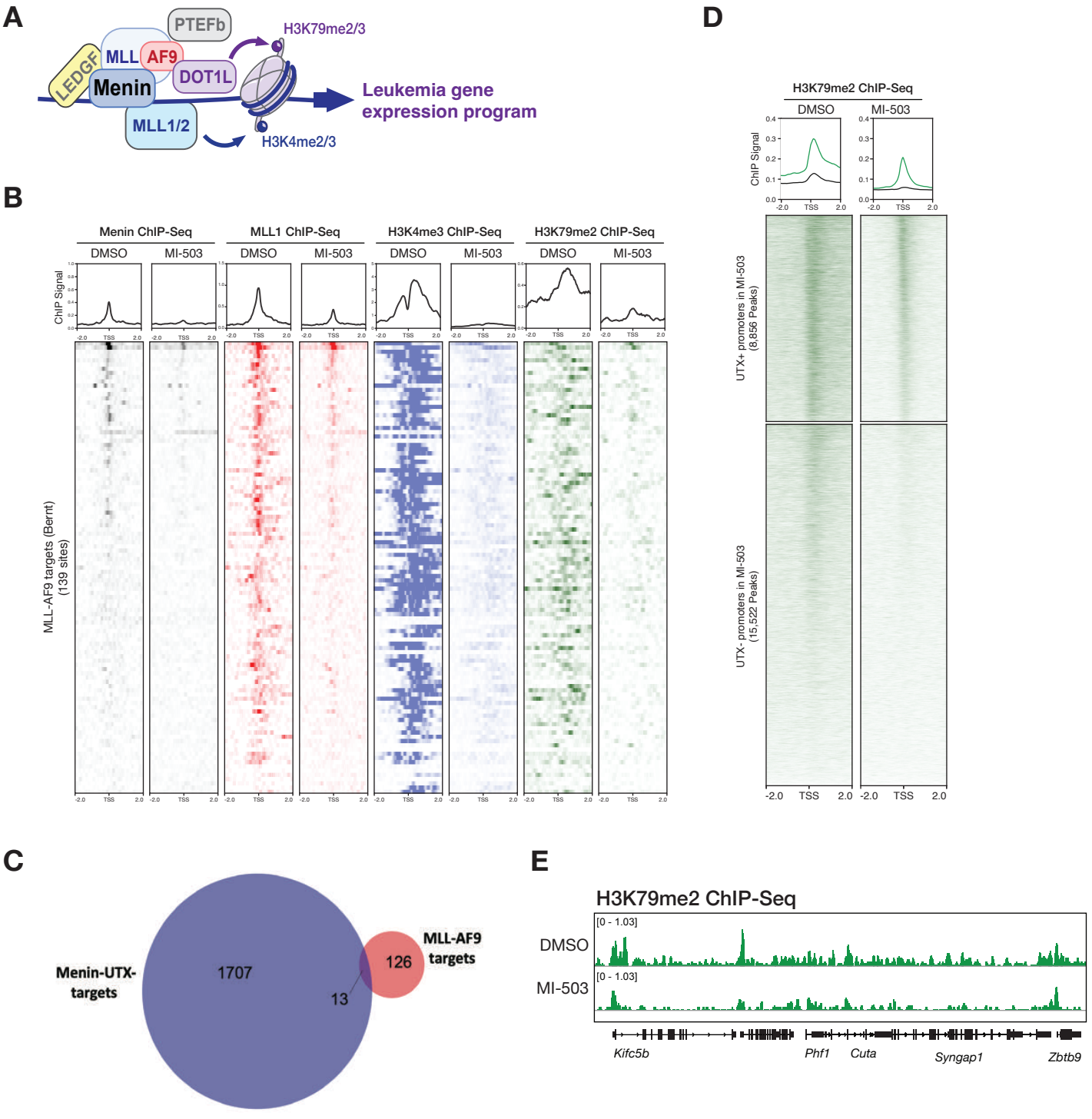


**Supplementary Figure 9. MLL1-Menin genomic targets are distinct from MLL-FP targets. (A)** Schematic representation of ectopic chromatin complexes that are formed by MLL-fusion proteins (MLL-FPs). **(B)** Heatmaps displaying Menin (black), MLL1 (red), H3K4me3 (blue), and H3K79me2 (green) ChIP-Seq signals mapping to MLL-AF9 target loci (139 sites) from MLL-AF9 leukemia cells treated with vehicle (DMSO) or Menin-MLL inhibitor (MI-503) for 96 hours. Metagene plot represents the average ChIP-Seq signal for each protein at promoters. **(C)** Overlap analysis between Menin-UTX and MLL-AF9 targets in leukemia cells. **(D)** Heatmaps displaying H3K79me2 ChIP-Seq signals mapping to a 4-kb window around TSSs in MLL-AF9 leukemia cells treated with vehicle (DMSO) or Menin-MLL inhibitor (MI-503) for 96 hours. Metaplot represents the average ChIP-Seq signal for H3K79me2 at promoters that are bound by UTX in MLL-AF9 cells treated with MI-503. **(E)** Genome browser representation of ChIP-Seq normalized reads for H3K79me2 in mouse MLL-AF9 leukemia cells treated with either vehicle (DMSO) or Menin-MLL inhibitor (MI-503) for 96 hours.

# SUPPLEMENTARY FIGURE 10

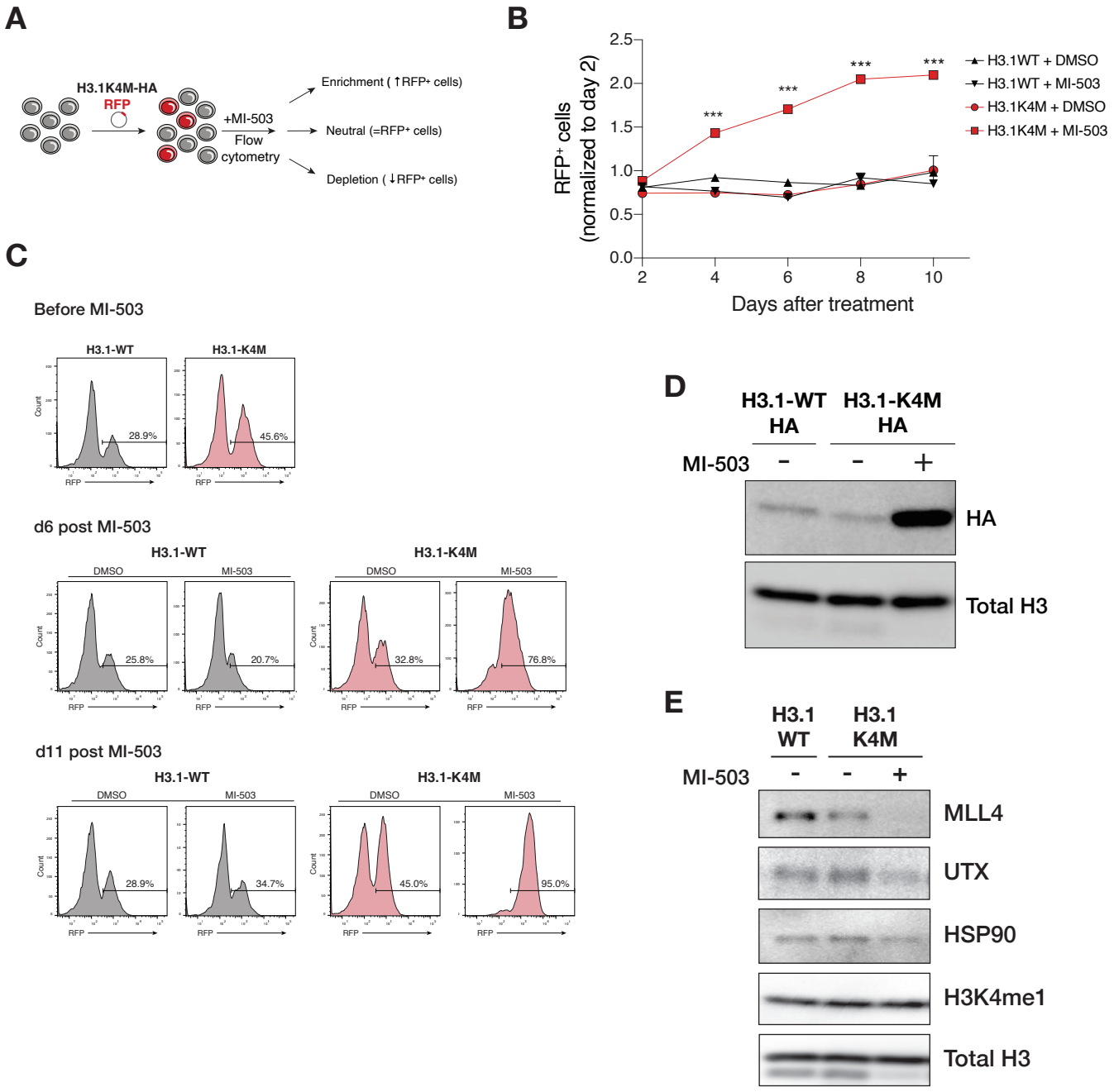


**Supplementary Figure 10. Destabilization of the MLL3/4-UTX complex is sufficient to blunt cellular responses to Menin-MLL inhibition. (A)** Layout of growth competition assay to assess the effects of expressing a H3.1K4M oncohistone mutation in MLL-AF9 leukemia cells in response to Menin-MLL inhibition. **(B)** Relative percentage of RFP+ transgene (H3.1WT or H3.1K4M) cells over time after transduction of mouse MLL-AF9 cells treated with vehicle (DMSO) or Menin-MLL inhibitor (MI-503) (mean±SEM, n=3 replicates, *P*-value calculated by Student's t-test, $P < 0.001$ = ***). **(C)** Expression of H3.1WT-RFP or H3.1K4M-RFP in mouse MLL-AF9 leukemia cells treated with DMSO or MI-503 was monitored by tracking RFP+ cells by flow cytometry over time. **(D)** Immunoblot analysis of HA-tag from MLL-AF9 leukemia cells expressing H3.1WT-HA or H3.1K4M-HA and treated with vehicle (DMSO) or Menin-MLL inhibitor (MI-503) for 6 days. **(E)** Immunoblot analysis of MLL4, UTX, HSP90 (loading control), H3K4me1, and total H3 (loading control) from MLL-AF9 leukemia cells expressing H3.1WT or H3.1K4M and treated with DMSO or MI-503 for 6 days.

# SUPPLEMENTARY FIGURE 11

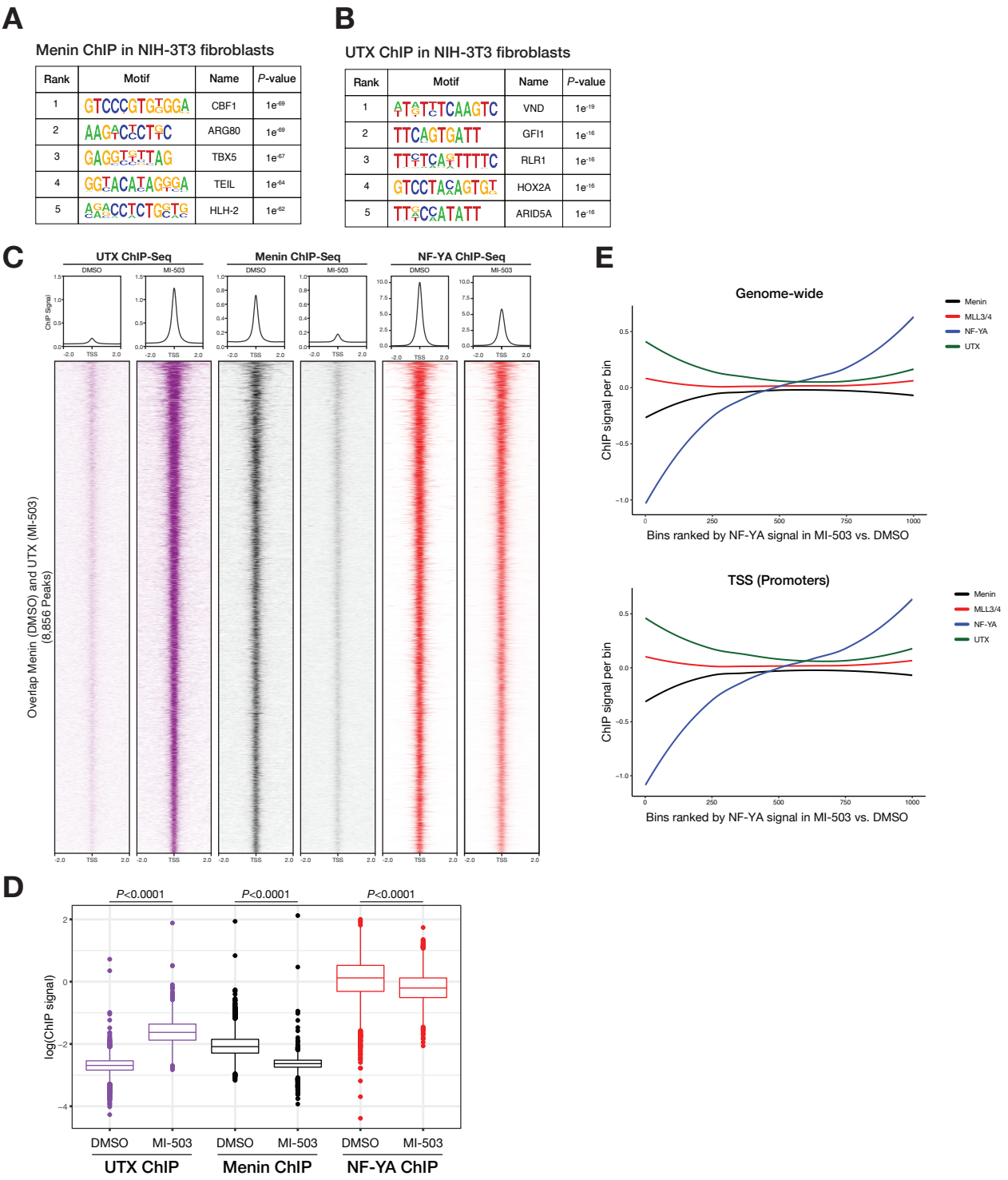


**Supplementary Figure 11. NF-Y restricts chromatin occupancy of UTX at promoter regions. (A)** Motif analysis of Menin ChIP-Seq peaks detected in NIH-3T3 mouse fibroblasts. **(B)** Motif analysis of UTX ChIP-Seq peaks detected in NIH-3T3 mouse fibroblasts. **(C)** Heatmaps displaying UTX (purple), Menin (black), and NF-YA (red) ChIP-Seq signals mapping to a 4-kb window around TSSs. Data is shown for vehicle (DMSO) and Menin-MLL inhibitor (MI-503)-treated cells for 96 hours. Metagene plot represents the average ChIP-Seq signal for each protein at promoters. **(D)** Boxplot showing ChIP signal changes for UTX (purple), Menin (black), and NF-YA (red) that are induced by Menin-MLL inhibitor (MI-503) treatment of mouse MLL-AF9 leukemia cells. *P*-value for MI-503 comparison is shown. **(E)** Line plots showing correlations between NF-YA (blue), Menin (black), MLL3/4 (red), and UTX (green) ChIP-Seq. NF-YA peaks are divided into bins and ranked by the NF-YA signal in MI-503 vs NF-YA signal in DMSO (relative to other ChIP signals).

# SUPPLEMENTARY FIGURE 12

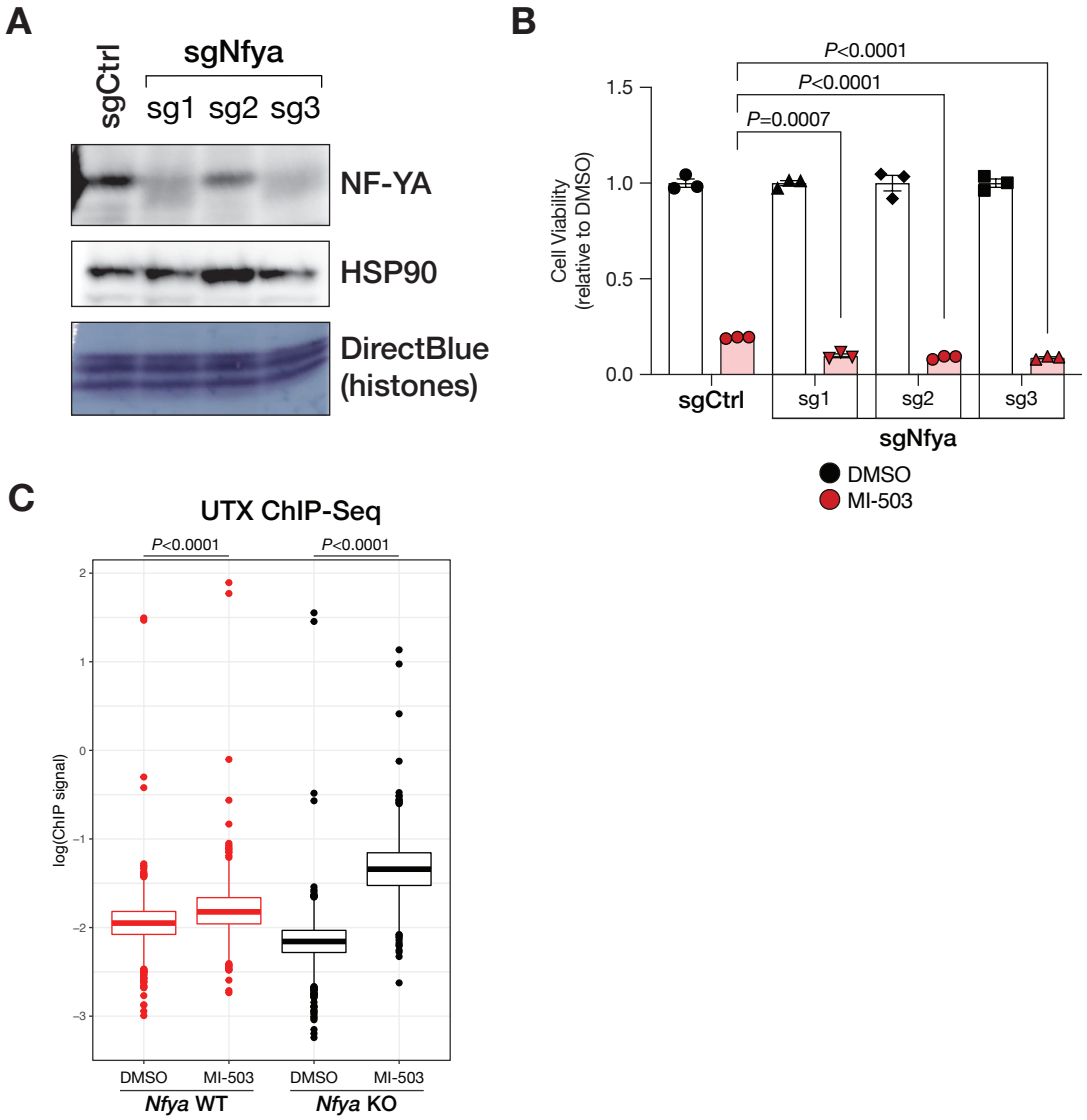


**Supplementary Figure 12. NF-Y facilitates promoter regulation by Menin. (A)** Immunoblot analysis of NF-YA and HSP90 proteins (loading control) in mouse MLL-AF9 leukemia cells transduced with a control sgRNA (sgCtrl) or three independent *Nfya*-targeting sgRNAs. Direct blue staining of histones (bottom) serves as an additional loading control. **(B)** Viability assay from cells treated with vehicle (DMSO, black) or Menin-MLL inhibitor (MI-503, red) for 6 days (mean±SEM, n=3 infection replicates, *P*-value calculated by Student's t-test). sgCtrl, control sgRNA targeting a non-genic region on chromosome 8. **(C)** Boxplot showing ChIP signal changes for UTX that are induced by Menin-MLL inhibitor (MI-503) treatment of *Utx*WT (red) and *Utx*KO (black) leukemia cells. *P*-value for MI-503 comparison is shown.

# SUPPLEMENTARY FIGURE 13

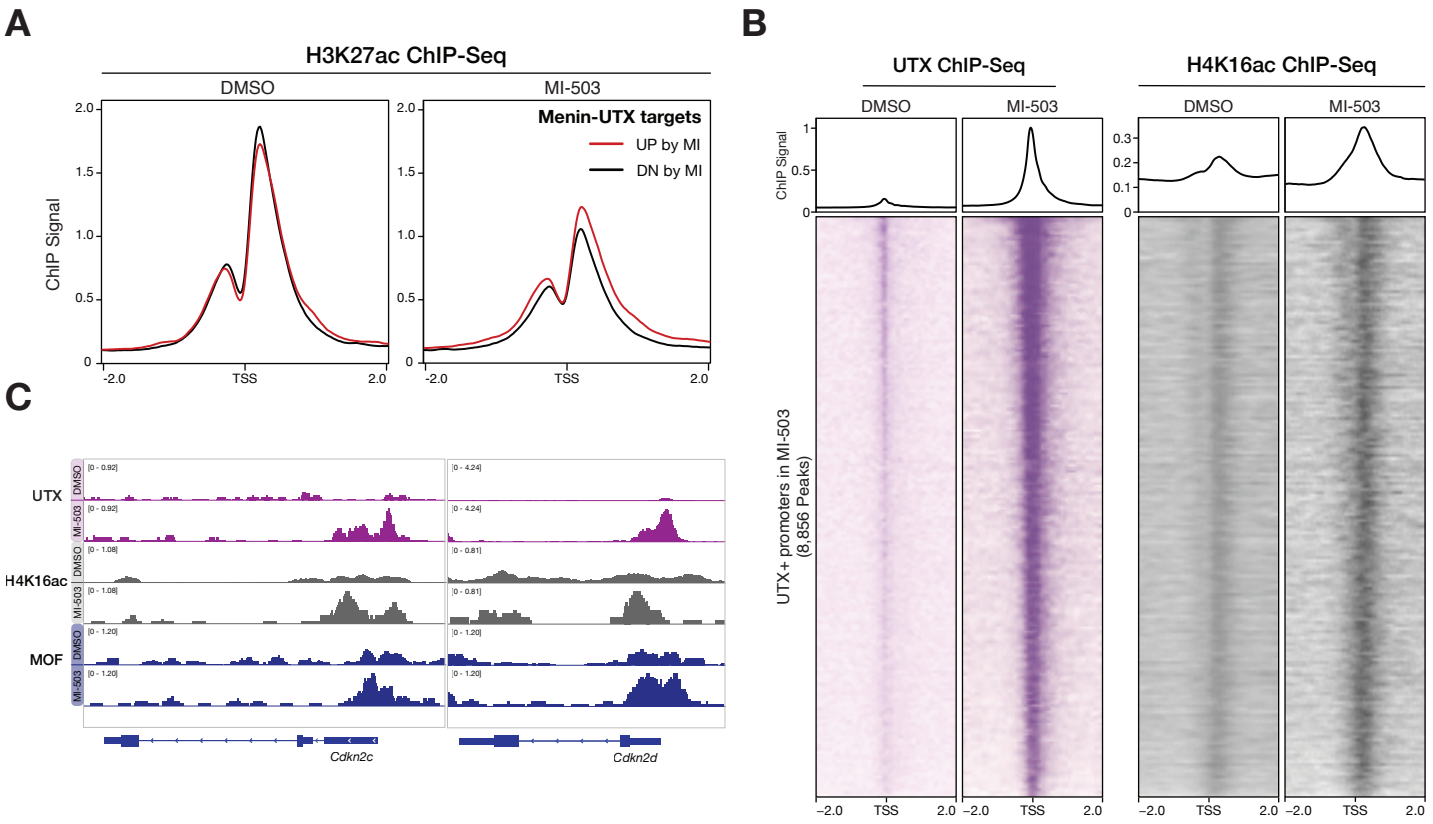


**Supplementary Figure 13. Menin-UTX molecular switch coincides with local changes in histone acetylation. (A)** Average ChIP-Seq signal for H3K27ac at transcription start sites (TSS) ±2kb of the Menin-UTX target genes. Signals corresponding to genes that are upregulated (red) or down-regulated (black) when cells are treated with Menin-MLL inhibitor (MI-503) for 96 hours. RPM, reads per million. **(B)** Heatmaps displaying UTX (purple) or H4K16ac (gray) ChIP-Seq signals mapping to a 4-kb window around TSSs in MLL-AF9 leukemia cells treated with vehicle (DMSO) or Menin-MLL inhibitor (MI-503) for 96 hours. Metagene plot represents the average ChIP-Seq signal for each protein at promoters that are bound by UTX in mouse MLL-AF9 leukemia cells treated with MI-503 for 96 hours. **(C)** Genome browser representation of ChIP-Seq normalized reads (average RPKM) for UTX (purple), H4K16ac (gray), and MOF (blue) at *Cdkn2c* and *Cdkn2d* loci from MLL-AF9 cells treated with DMSO or MI-503 for 96 hours.

# SUPPLEMENTARY FIGURE 14

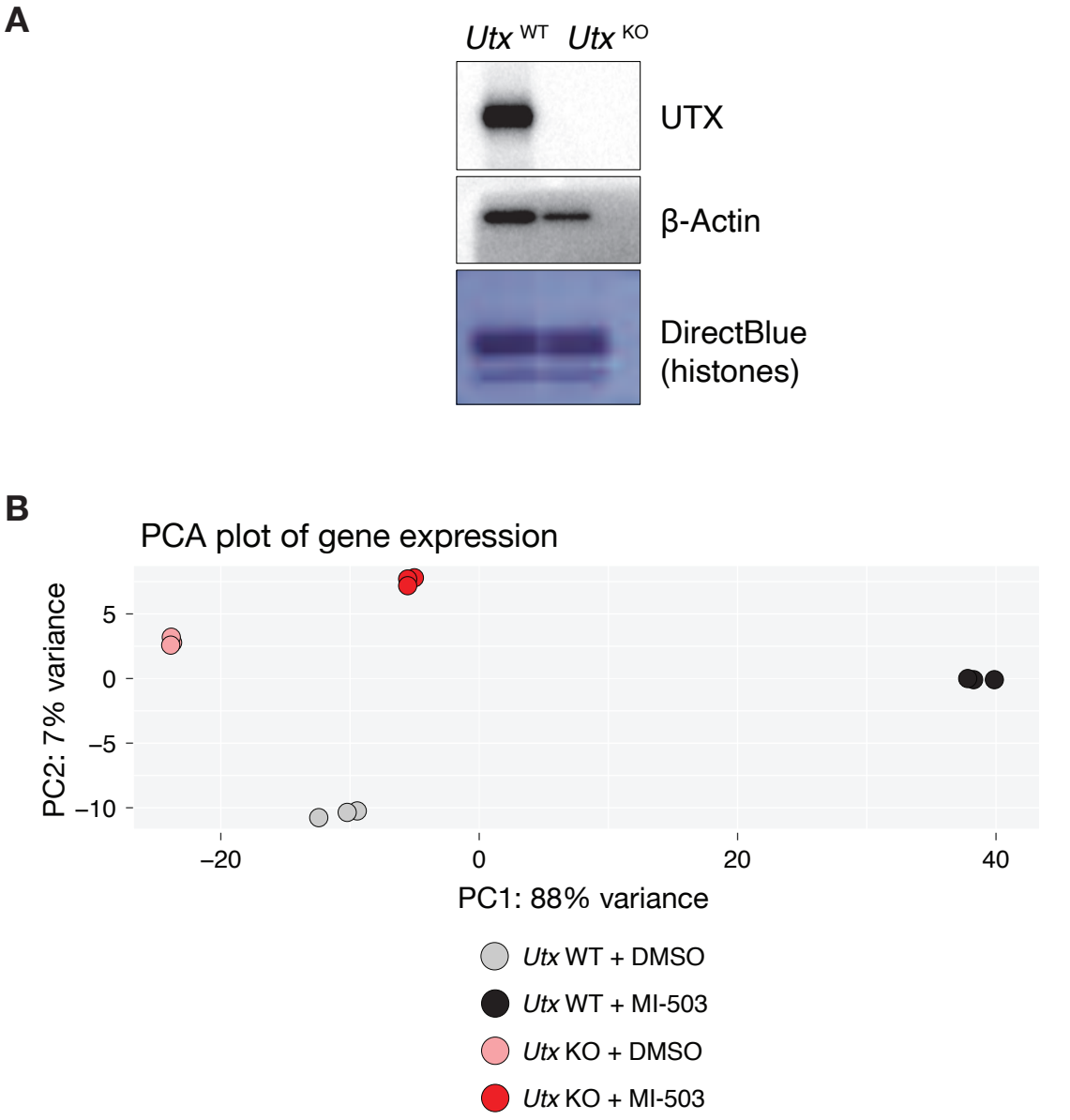


**Supplementary Figure 14. Transcriptional assessment of UtxKO MLL-AF9 leukemia cells. (A)** Immunoblot analysis of UTX and β-actin (loading control) from mouse *Utx*$^{WT}$ and *Utx*$^{KO}$ MLL-AF9 leukemia cells. **(B)** Principal component analysis (PCA) using RNA-Seq gene expression data from *Utx*$^{WT}$ and *Utx*$^{KO}$ cells treated with vehicle (DMSO) or Menin-MLL inhibitor (MI-503) for 96 hours.

# SUPPLEMENTARY FIGURE 15

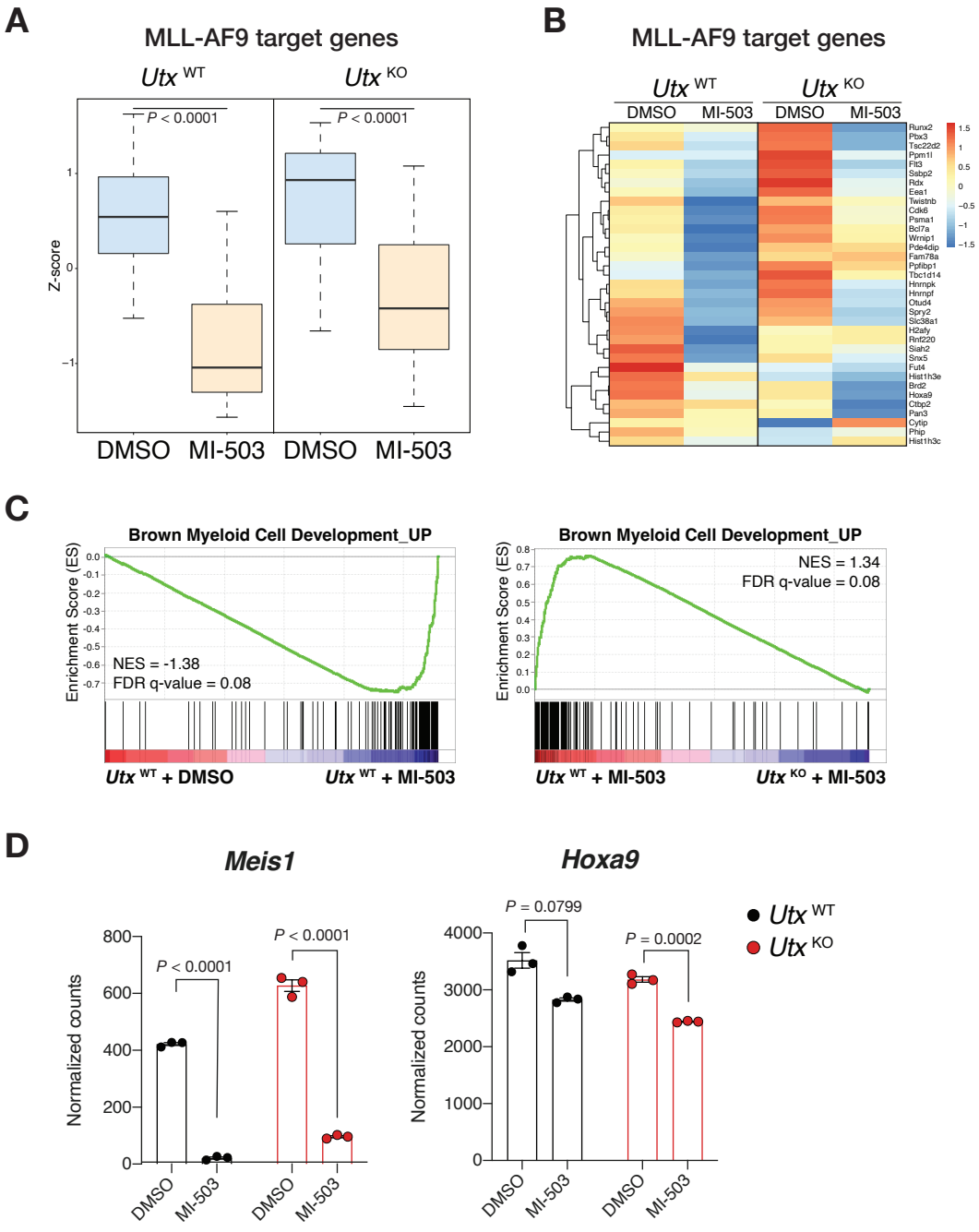


**Supplementary Figure 15. MLL-AF9 target genes are not regulated by the Menin-UTX molecular switch. (A)** Boxplot showing expression levels of MLL-AF9 target genes, which are suppressed by the Menin-MLL inhibitor (MI-503) treatment for 96 hours. Expression levels are shown for *Utx*$^{WT}$ (left) and *Utx*$^{KO}$ (right) mouse leukemia cells. *P*-value calculated by Student's t-test). **(B)** Heatmap of Z-scores for expression of MLL-AF9 target genes from *Utx*$^{WT}$ and *Utx*$^{KO}$ leukemia cells treated with DMSO or MI-503 for 96 hours. **(C)** GSEA plots showing changes in regulation of myeloid cell differentiation in genes induced by MI-503 for 96 hours. FDR, false discovery rate; NES, normalized enrichment score. **(D)** *Meis1* (left) and *Hoxa9* (right) expression (mean normalized read counts) from *Utx*$^{WT}$ and *Utx*$^{KO}$ leukemia cells treated with DMSO or MI-503 for 96 hours (mean±SEM, n=3 replicates, *P*-value calculated by Student's t-test).

# SUPPLEMENTARY FIGURE 16

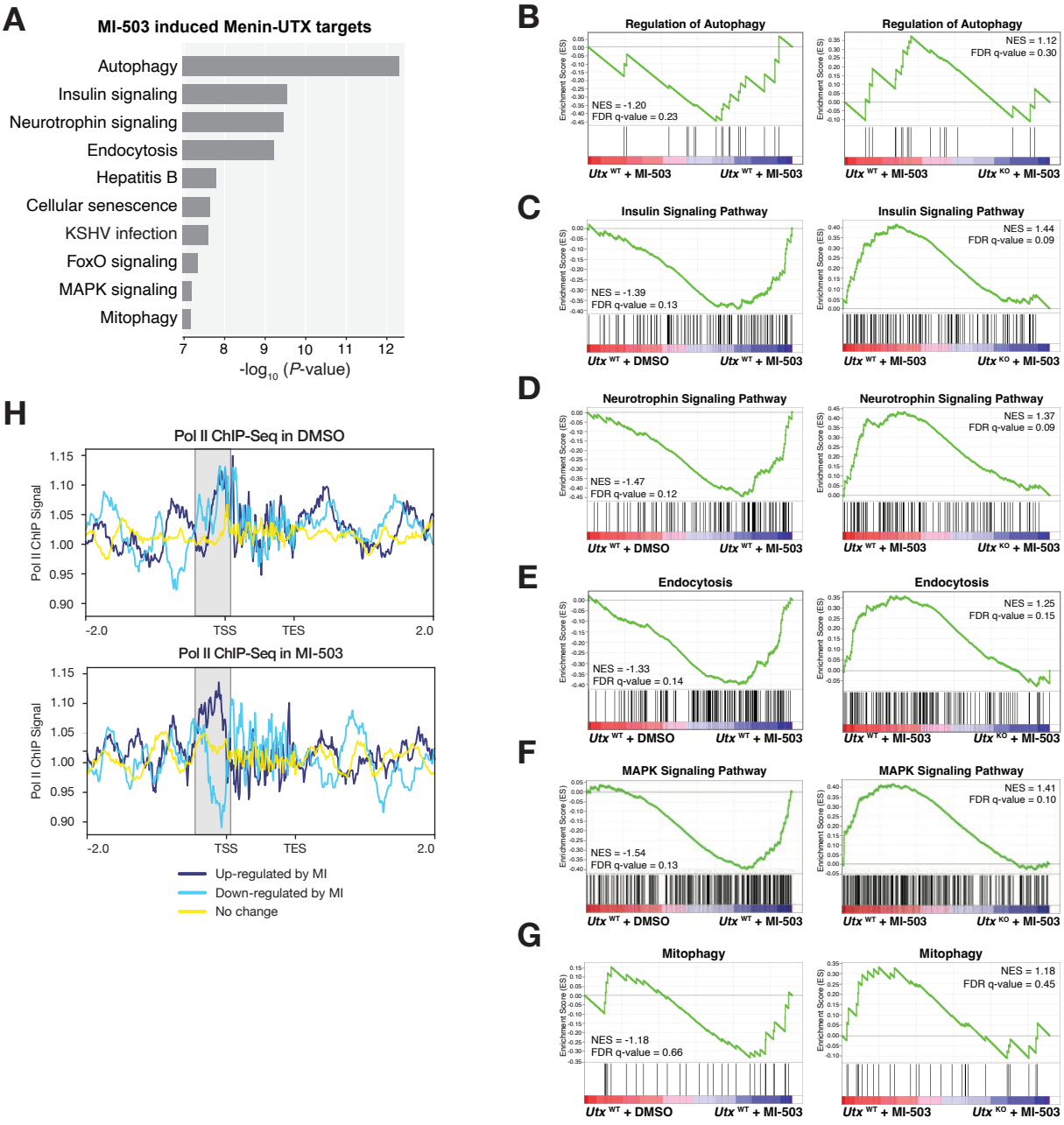


**Supplementary Figure 16. Gene sets and pathways regulated by Menin-UTX molecular switch.** **(A)** Gene ontology (GO) analysis of Menin-UTX targets using expression data from mouse MLL-AF9 leukemia cells treated with vehicle (DMSO) or Menin-MLL (MI-503) for 96 hours. Top 10 GO categories sorted based on statistical significance are shown. **(B)** GSEA plots showing changes in regulation of autophagy genes induced by MI-503 treatment for 96 hours. FDR, false discovery rate; NES, normalized enrichment score. **(C)** GSEA plots showing changes in insulin signaling pathway genes induced by MI-503 treatment for 96 hours. **(D)** GSEA plots showing changes in neurotrophin signaling pathway genes induced by MI-503 treatment for 96 hours. **(E)** GSEA plots showing changes in endocytosis genes induced by MI-503 treatment for 96 hours. **(F)** GSEA plots showing changes in MAPK signaling pathway genes induced by MI-503 treatment for 96 hours. **(G)** GSEA plots showing changes in mitophagy genes induced by MI-503 treatment for 96 hours. **(H)** RNA Pol II ChIP-Seq signal determined for senescence and cell-cycle arrest-associated genes that are Menin-UTX targets.

# SUPPLEMENTARY FIGURE 17

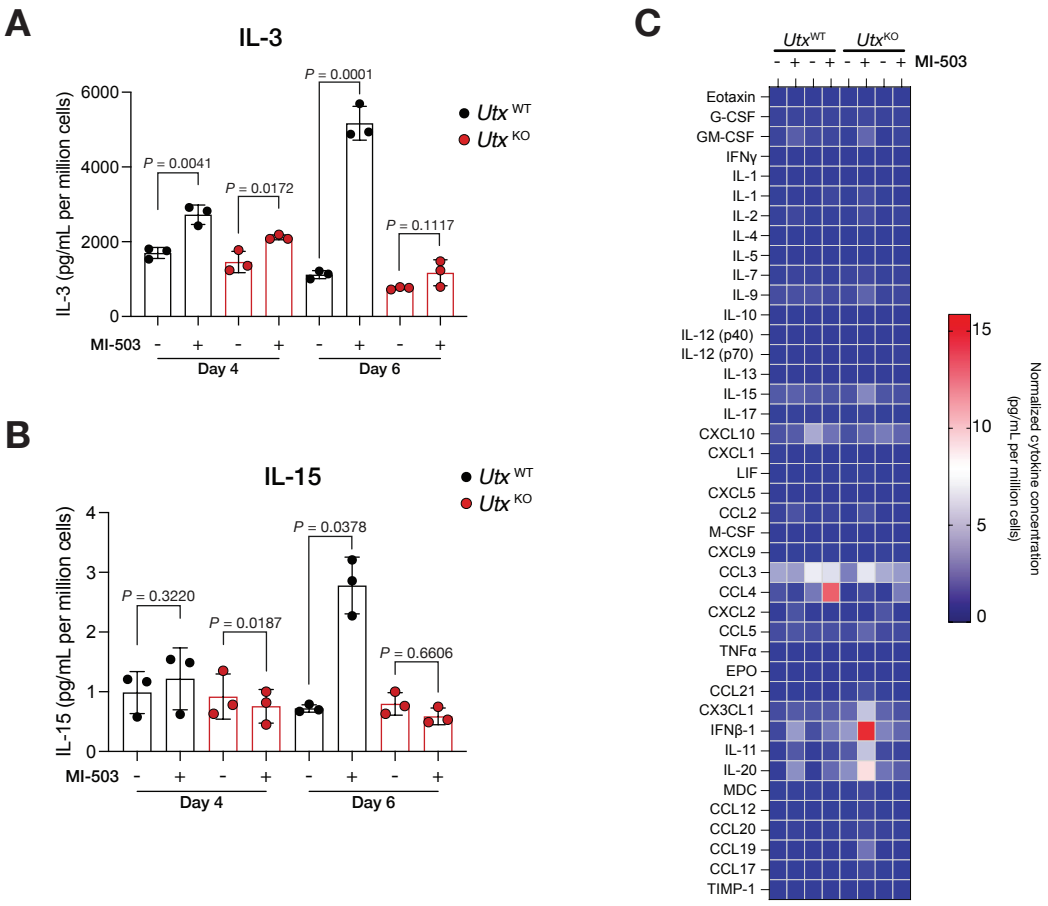


**Supplementary Figure 17. MLL3/4-UTX-dependent induction of SASP cytokines upon Menin-MLL inhibition. (A)** Secreted levels of IL-3 in mouse UtxWT and UtxKO MLL-AF9 leukemia cells treated with Menin inhibitor (MI-503) or vehicle (DMSO) after four or six days. Data are quantified as pg/mL of secreted cytokine per million cells (mean±SEM, n=3 replicates, *P*-value calculated by Student's t-test). **(B)** Secreted levels of IL-15 in *Utx*$^{WT}$ and *Utx*$^{KO}$ MLL-AF9 leukemia cells treated with Menin inhibitor (MI-503) or vehicle (DMSO) after four or six days. Data are quantified as pg/mL of secreted cytokine per million cells (mean±SEM, n=3 replicates, *P*-value calculated by Student's t-test). **(C)** Heatmap of cytokine array results from *Utx*$^{WT}$ and *Utx*$^{KO}$ MLL-AF9 leukemia cells treated with Menin inhibitor (MI-503) or vehicle (DMSO) after four or six days. Data are quantified as pg/mL of secreted cytokine per million cells and represent the mean of three biological replicates. Note that the very high levels of IFNβ-1 secretion relative to the rest of the cytokines measured affect the dynamic range of data visualization.

# SUPPLEMENTARY FIGURE 18

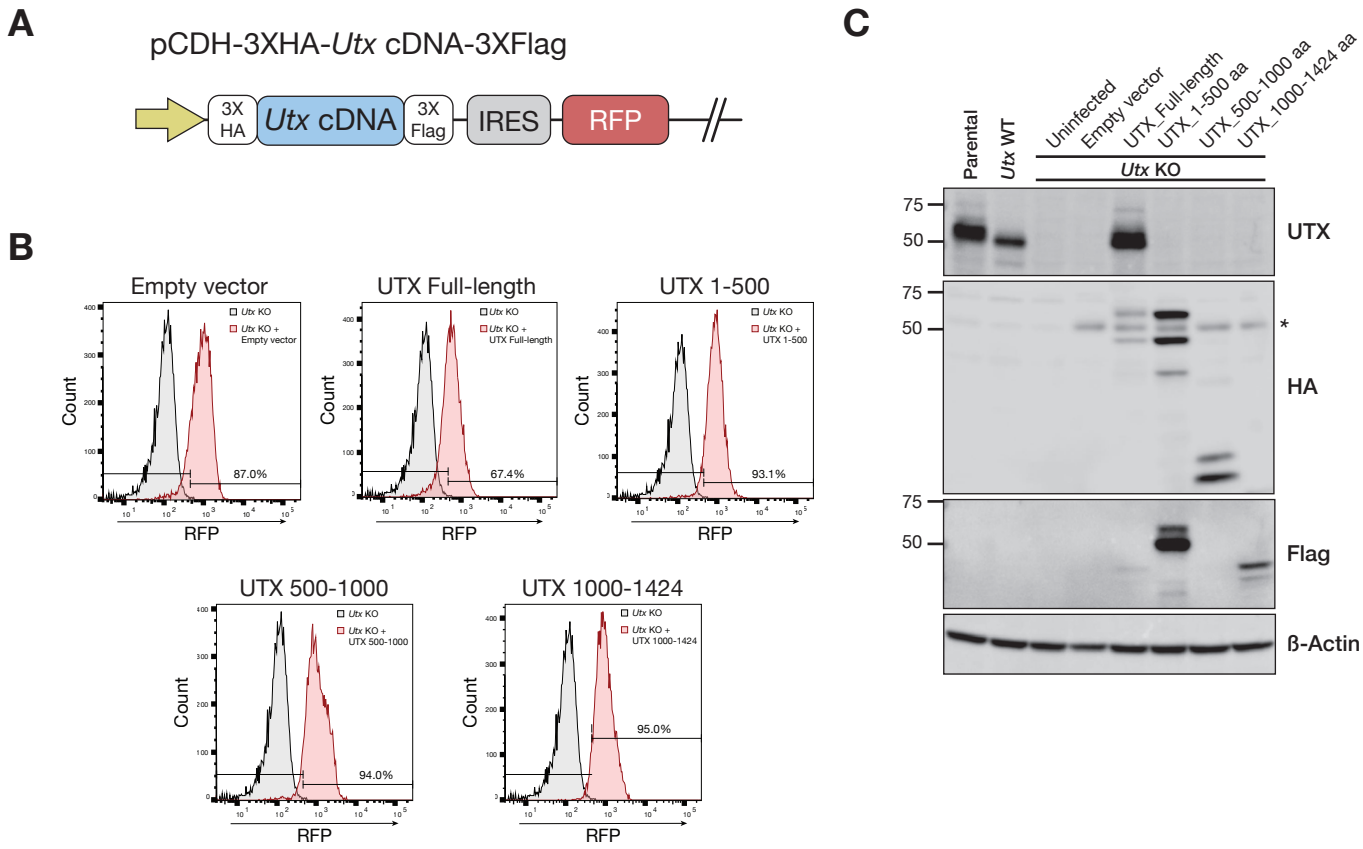


**Supplementary Figure 18. Expression of UTX truncations in MLL-AF9 *Utx*$^{KO}$ leukemia cells. (A)** Representation of the lentiviral vector used to stably co-express N-terminal HA-/C-terminal-Flag-tagged *Utx* cDNAs and the fluorescent protein RFP. **(B)** Flow cytometry plots showing RFP expression of the different mouse MLL-AF9 leukemia cell lines generated with the *Utx* truncations. **(C)** Immunoblotting validation of expression of the different *Utx* truncations in mouse MLL-AF9 leukemia cells using antibodies against UTX, HA-tag, Flag-tag, and β-actin (loading control).

# SUPPLEMENTARY FIGURE 19

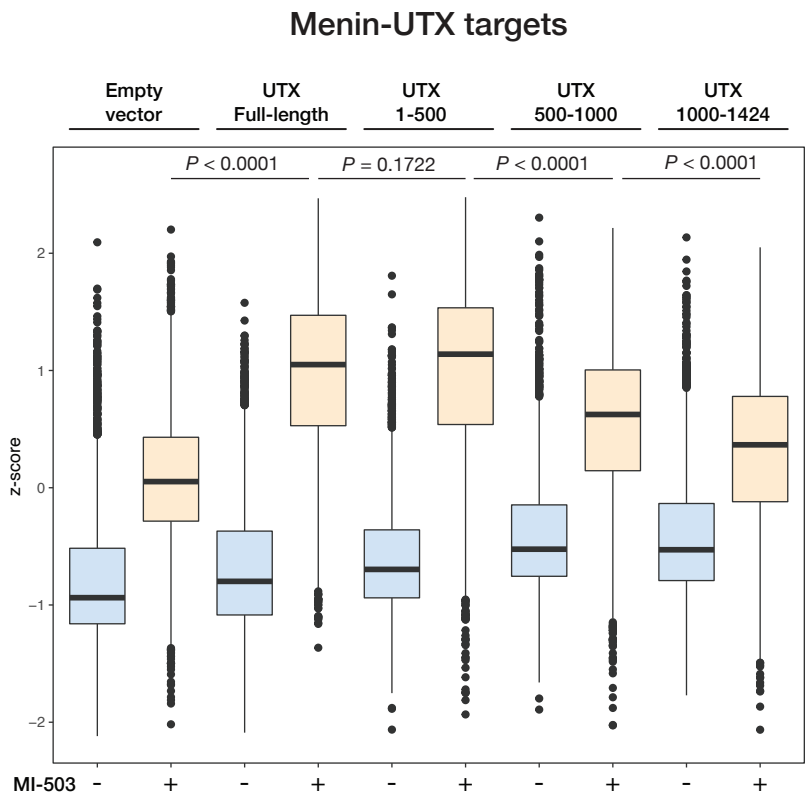


**Supplementary Figure 19. Transcriptional characterization of the different *Utx* truncations in mouse MLL-AF9 leukemia cells.** Boxplot showing expression levels of Menin-UTX target genes in mouse MLL-AF9 leukemia cells treated with vehicle (DMSO) or Menin-MLL inhibitor (MI-503) for 96 hours.

# SUPPLEMENTARY FIGURE 20

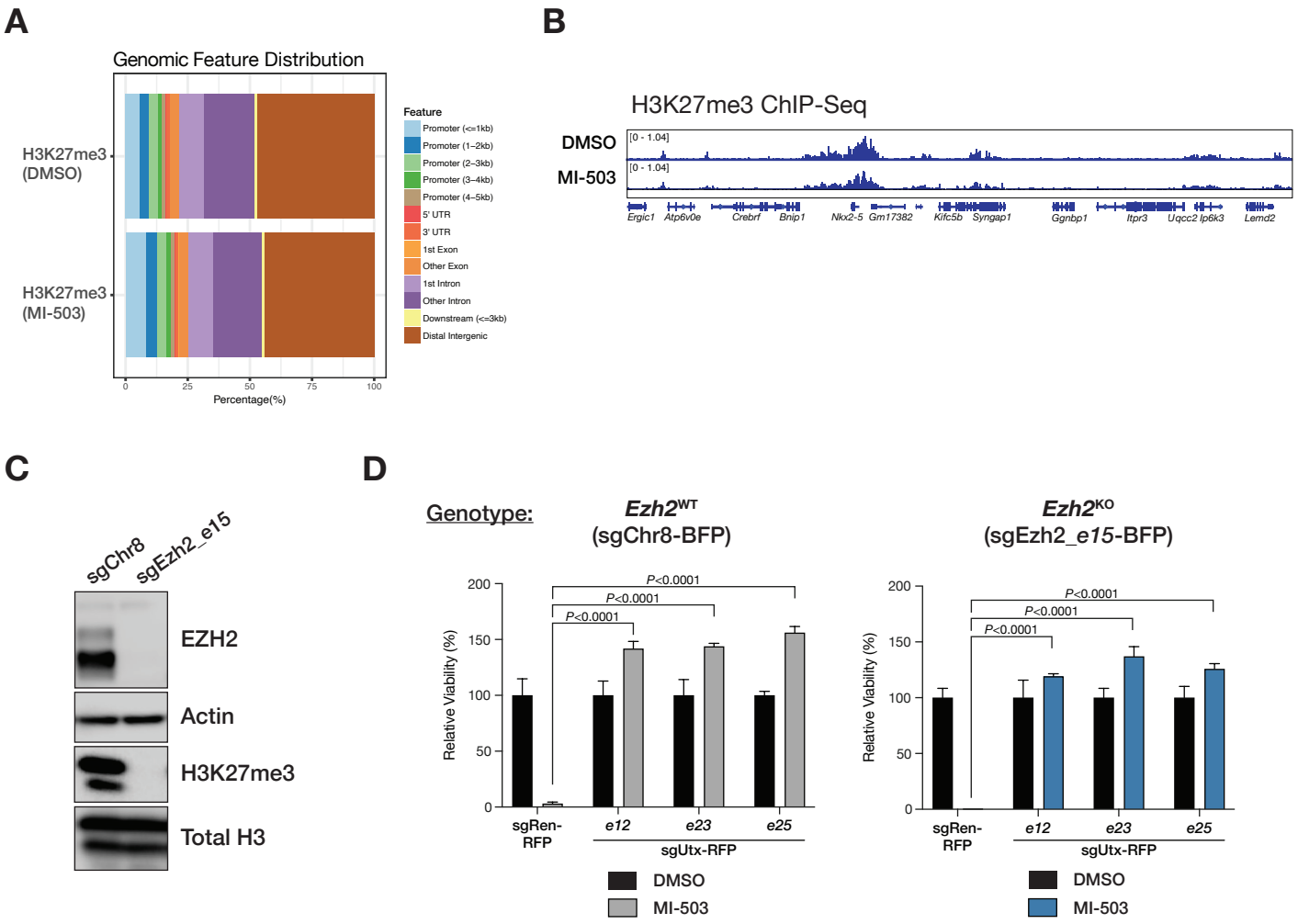


**Supplementary Figure 20. UTX-dependent phenotypes are not associated with global changes in H3K27 methylation. (A)** Genomic distribution of H3K27me3 ChIP-Seq peaks from mouse leukemia cells treated with vehicle (DMSO) or Menin-MLL inhibitor (MI-503) for 96 hours. **(B)** Genome browser representation of ChIP-Seq normalized reads (average RPKM) for H3K27me3 from MLL-AF9 cells treated with DMSO or MI-503 for 96 hours. **(C)** Immunoblot analysis of EZH2, β-actin (loading control), H3K27me3, and total H3 (loading control) from *Ezh2*$^{WT}$ and *Ezh2*$^{KO}$ mouse MLL-AF9 leukemia cells. **(D)** Viability assay from mouse *Ezh2*$^{WT}$ (left) and *Ezh2*$^{KO}$ (right) MLL-AF9 leukemia cells treated with vehicle (DMSO, black) or Menin-MLL inhibitor (MI-503, gray or blue) for 96 hours (mean±SEM, n=3 infection replicates, *P*-value calculated by Student's t-test). sgCtrl, control sgRNA targeting a non-genic region on chromosome 8.

# SUPPLEMENTARY FIGURE 21

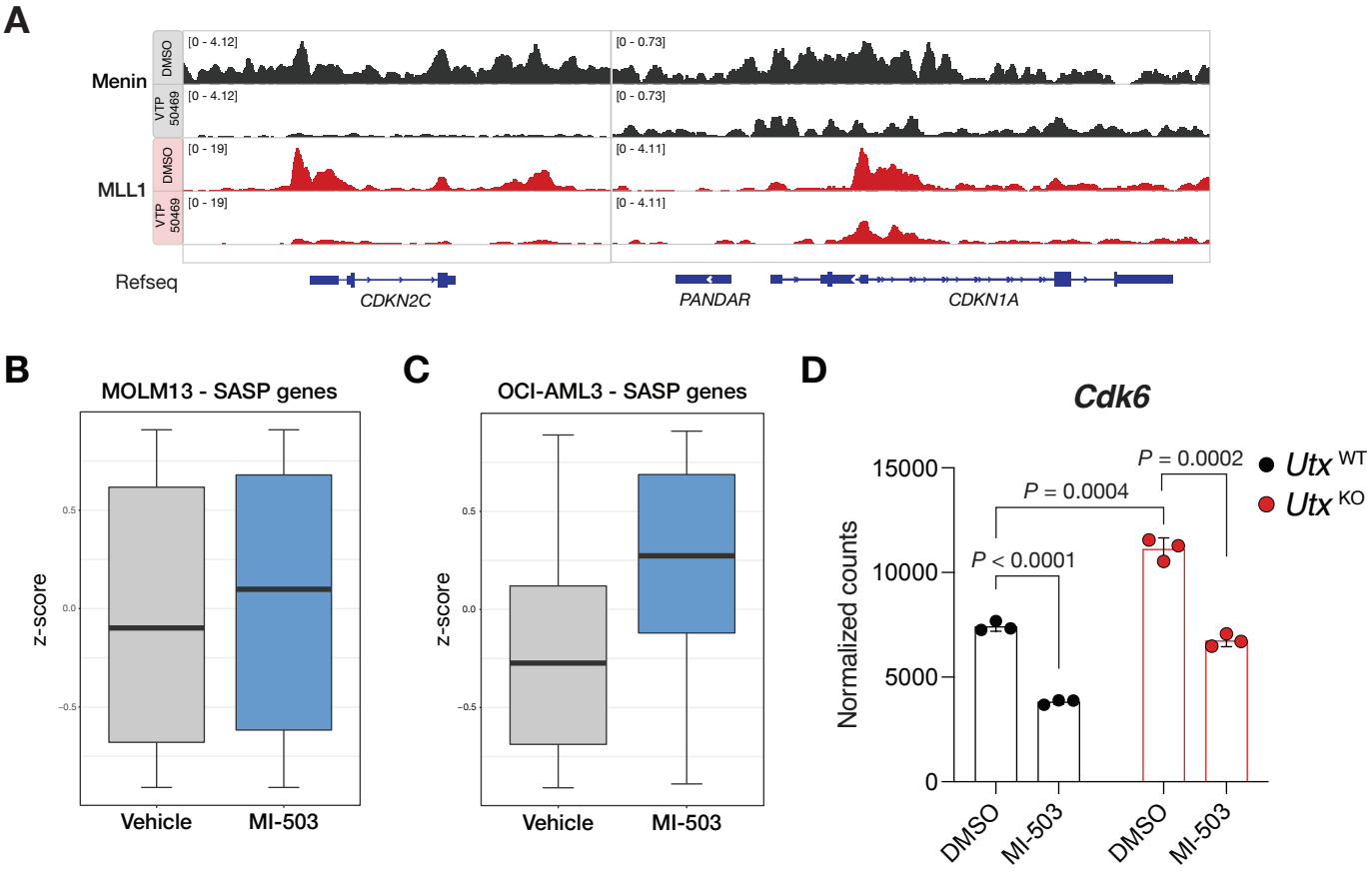


**Supplementary Figure 21. Induction of the Menin-UTX molecular switch upon Menin-MLL1 inhibition in human leukemia cells. (A)** Genome browser representation of ChIP-Seq normalized reads (average RPKM) for Menin (black) or MLL1 (red) at *CDKN2C* and *CDKN1A* loci from MOLM13 human leukemia cells treated with vehicle (DMSO) or Menin-MLL inhibitor (VTP-50469) for 7 days. **(B)** Boxplot showing expression levels of SASP genes in MOLM13 human leukemia cells treated with DMSO or MI-503 for 96 hours. **(C)** Boxplot showing expression levels of SASP genes in OCI-AML3 human leukemia cells treated with DMSO or MI-503 for 96 hours. **(D)** *Cdk6* expression (mean normalized read counts) from *Utx*$^{WT}$ (black) and *Utx*$^{KO}$ (red) leukemia cells treated with DMSO or MI-503 for 96 hours (mean±SEM, n=3 replicates, *P*-value calculated by Student's t-test).

# SUPPLEMENTARY FIGURE 22

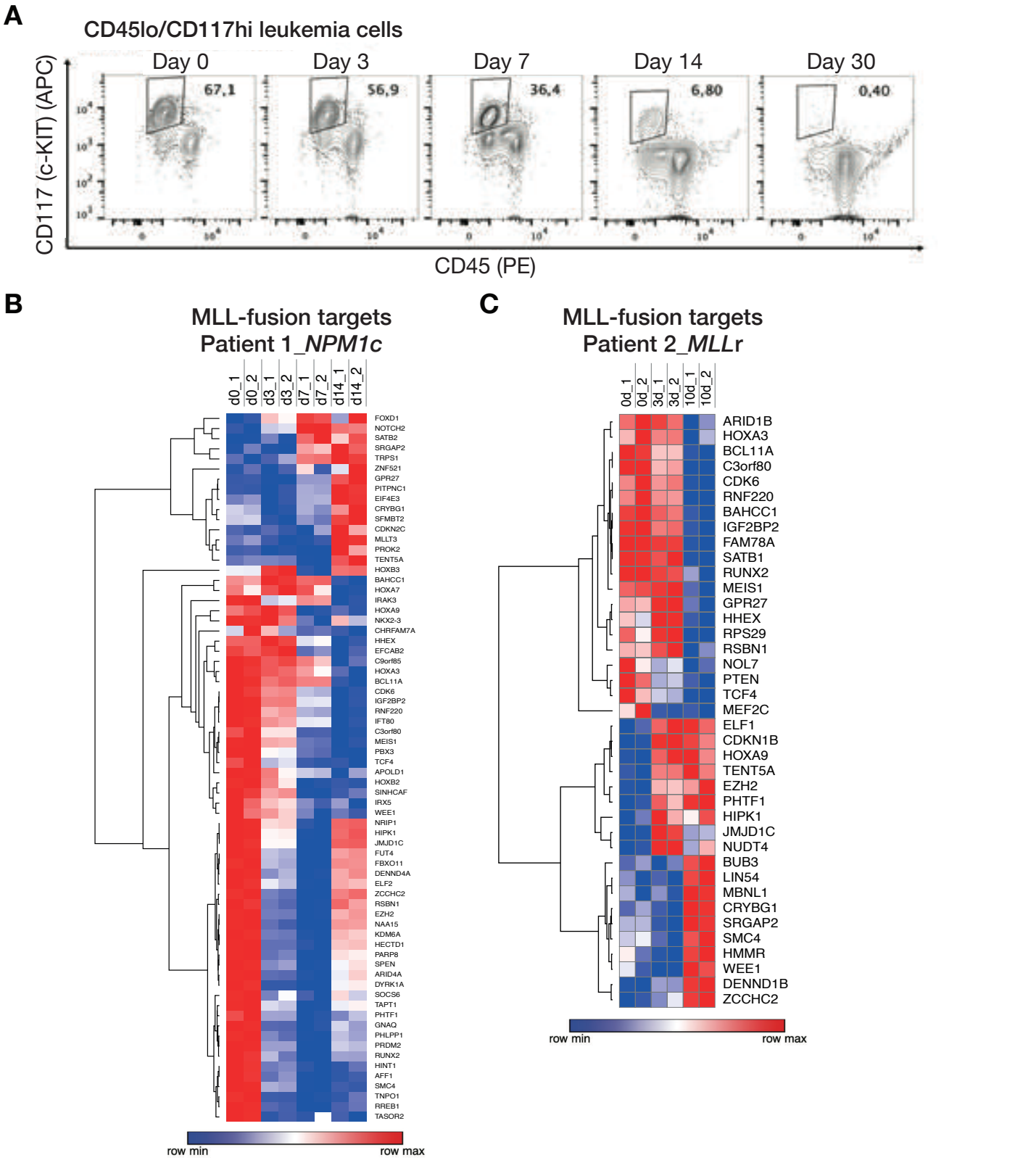


**Supplementary Figure 22. Characterization of primary human AML samples from patients participating in the Syndax Phase I Menin-MLL inhibitor trial. (A)** Immunophenotyping of primary human AML cells isolated from Patient 1 (*NPM1c* mutant AML). **(B)** Heatmap representation of Z-scores from longitudinal gene expression analysis of AML cells derived from Patient 1 (*NPM1c* mutant AML) treated with SNDX-5613. Displayed are MLL-AF9 target genes (Olsen et al. Mol.Cell, 2022) that are differentially expressed (padj<0.05, FC>2) in the dataset. **(C)** Heatmap representation of Z-scores from longitudinal gene expression analysis of AML cells derived from Patient 2 (*MLL*-rearranged AML) treated with SNDX-5613. Displayed are MLL-AF9 target genes (Olsen et al. Mol.Cell, 2022) that are differentially expressed (*P*-adj<0.05, FC>2) in the dataset.

# SUPPLEMENTARY FIGURE 23

**A**

| PDX Sample | *MLL*-r | *MLL3* status |
|---|---|---|
| DFAM68555 | MLL-AF9 | wild-type |
| MSK042D | MLL-AF4 | mutant |

**B**

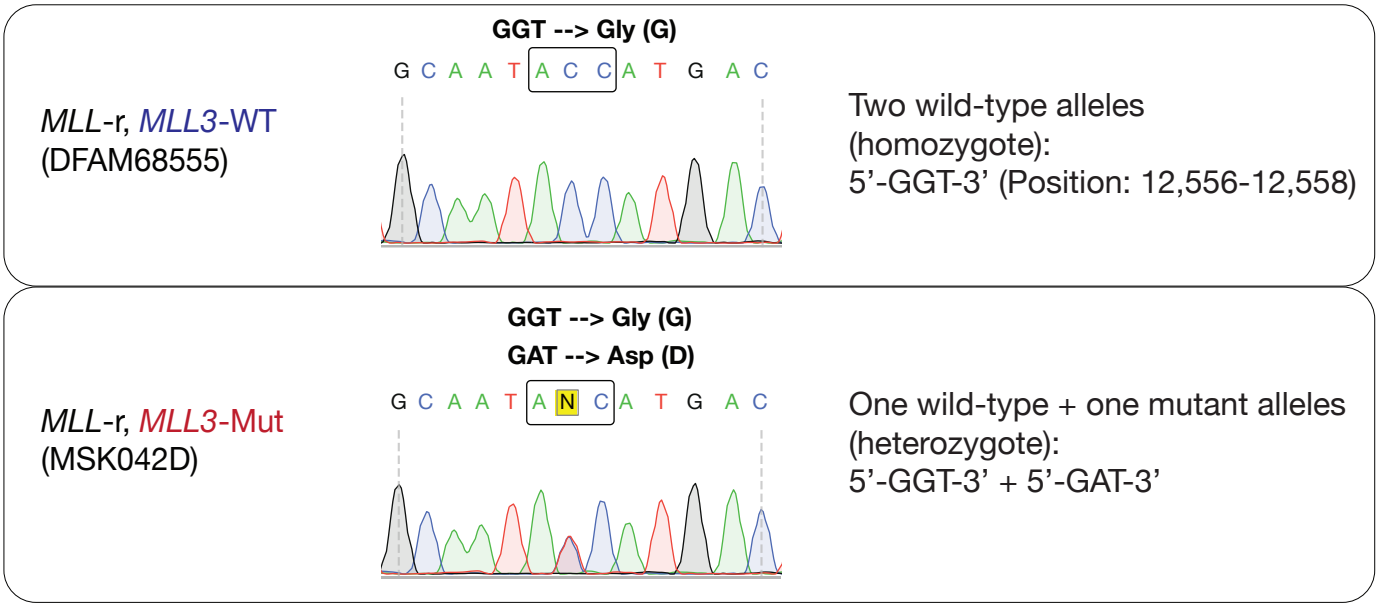


**Supplementary Figure 23. Modeling of Menin-MLL inhibitor response in patient-derived xenografts. (A)** Characteristics of *MLL*-r AML PDX samples analyzed in this study. **(B)** Targeted sequencing validation of MLL3 status in PDX samples.

# SUPPLEMENTARY FIGURE 24

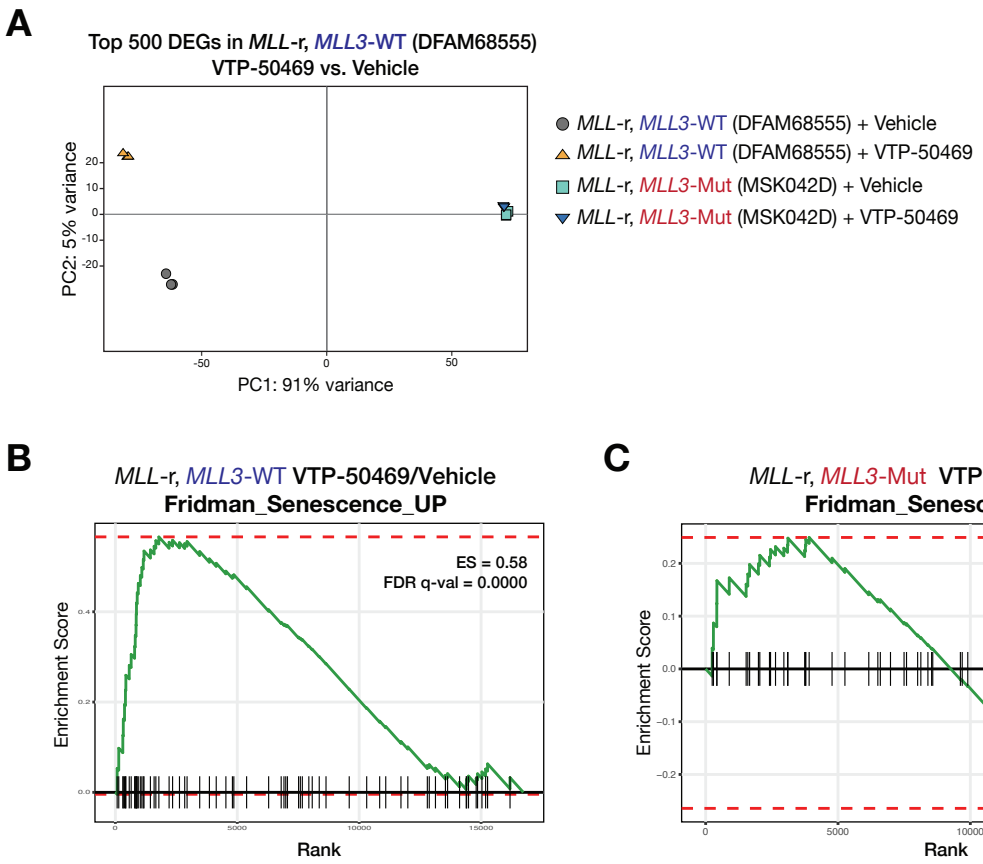


**Supplementary Figure 24. Transcriptional characterization of Menin-MLL inhibitor response in patient-derived xenografts. (A)** PCA using gene expression data obtained from *MLL3*-WT (DFAM68555) and *MLL3*-Mutant (MSK042D) PDX samples treated with vehicle (DMSO) or Menin-MLL inhibitor (VTP-50469). Analysis was performed using the top 500 differentially-expressed genes upon treatment of *MLL3*-WT PDXs with VTP-50469. Note that *MLL3*-Mutant PDX samples are virtually overlapping independent of the condition, suggesting that the induction of the Menin-UTX molecular switch is impaired in the context of MLL3 mutation. **(B)** GSEA showing that Menin-MLL inhibition using VTP-50469 leads to induction of cellular senescence in *MLL3*-WT PDX. **(C)** GSEA showing that Menin-MLL inhibition using VTP-50469 fails to induce cellular senescence in MLL3-Mutant PDX.

# SUPPLEMENTARY FIGURE 25

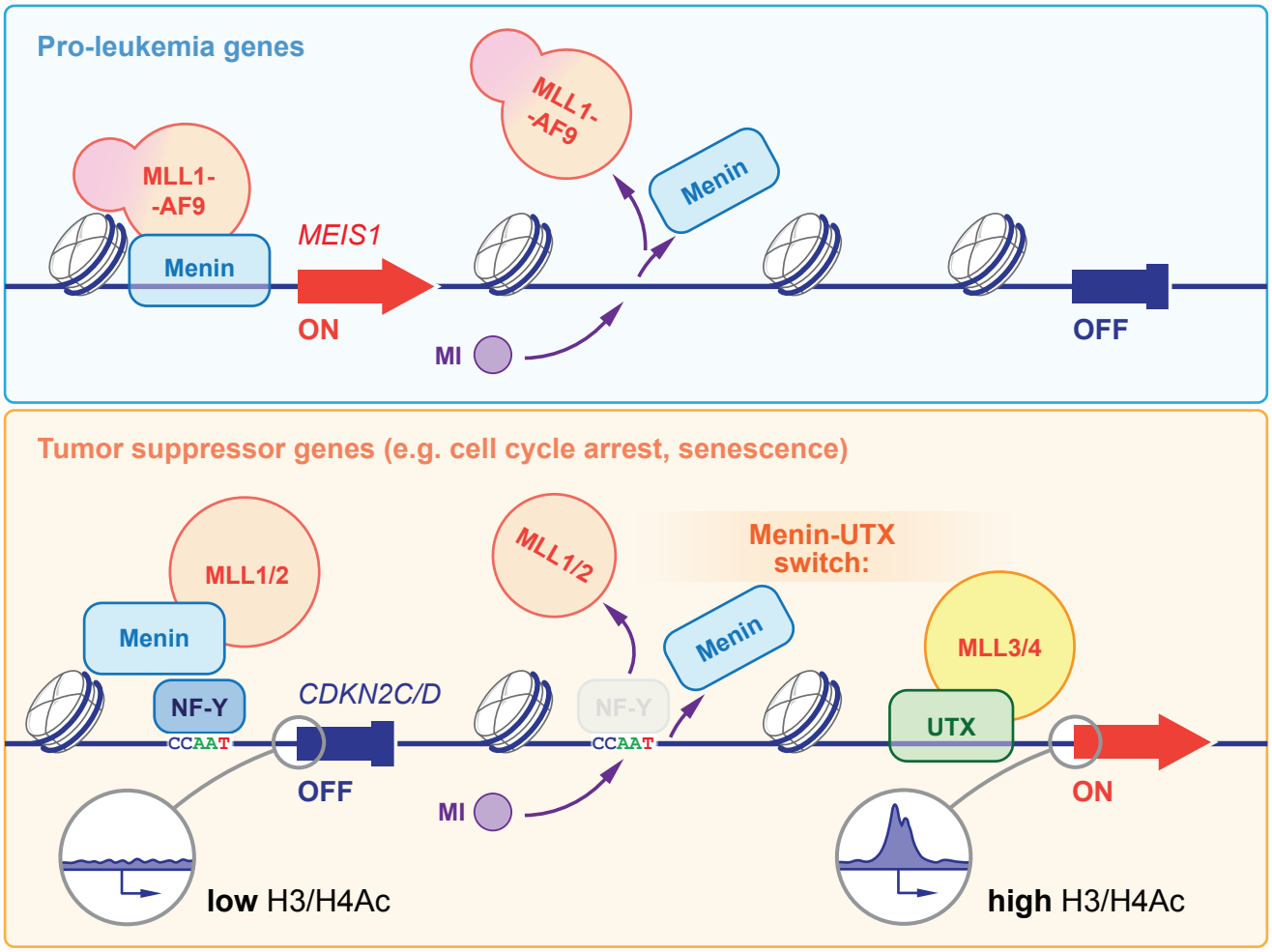


**Supplementary Figure 25. Molecular switch between the mammalian MLL complexes dictates cellular response to Menin-MLL inhibition.**